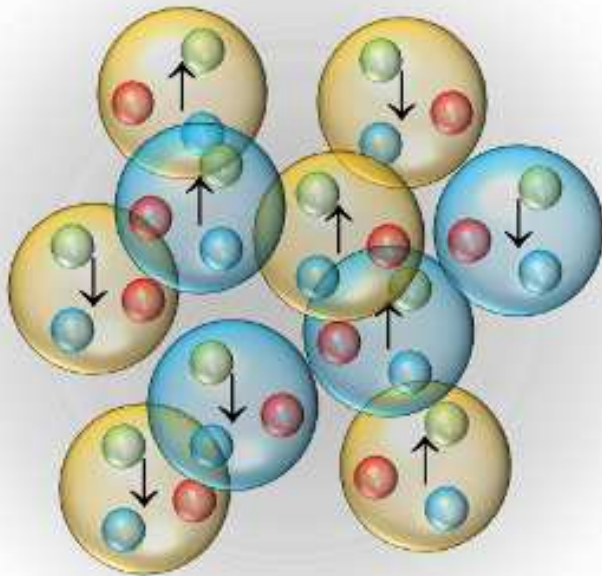


Insight into the structure of light nuclei through short- and long-range correlations



Thomas Neff
INT Workshop
“Structure of Light Nuclei”
Seattle, USA
October 8-12, 2012

Overview



Two-body densities in (very) light Nuclei

Unitary Correlation Operator Method

Fermionic Molecular Dynamics

$^3\text{He}(\alpha, \gamma)^7\text{Be}$ Radiative Capture Reaction

- bound and scattering states
- astrophysical S -factor

Cluster States in ^{12}C

- FMD and microscopic cluster model
- form factors, expansion in HO basis, two-body densities

Short-Range Correlations



Two-body densities for $A=2-4$ nuclei from few-body calculations with AV8' interaction

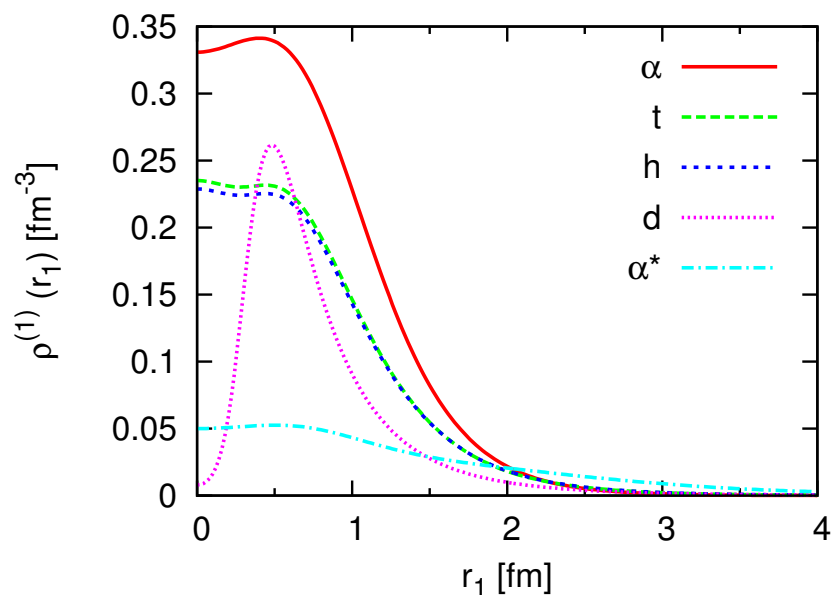
preliminary:

Two-body densities for ${}^4\text{He}$ using NCSM and SRG evolved AV18 interactions

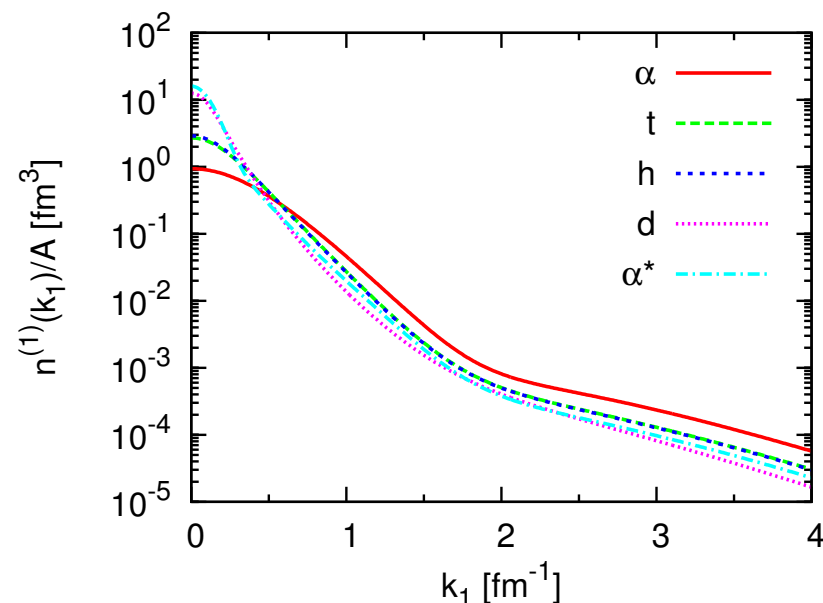
Two-body densities for ${}^4\text{He}$ using NCSM, SRG evolved AV18 and N3LO interactions and SRG transformed two-body density operators

- Short-range correlations
- One-body densities (AV8')

coordinate space



momentum space

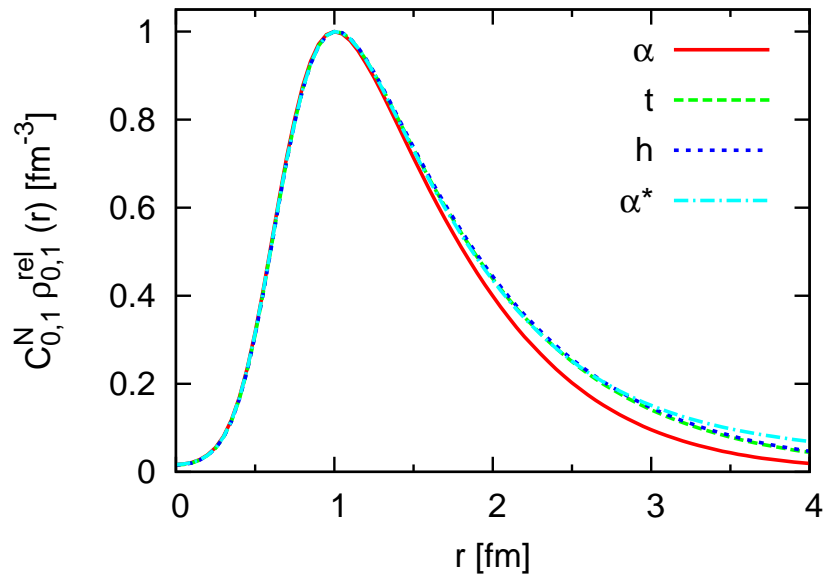


- one-body densities calculated from exact wave functions (Correlated Gaussians) for AV8' interaction
- coordinate space densities reflect different sizes and densities of ${}^2\text{H}$, ${}^3\text{H}$, ${}^3\text{He}$, ${}^4\text{He}$ and the 0_2^+ state in ${}^4\text{He}$
- similar high-momentum tails in the one-body momentum distribution

- Short-range correlations
- **Two-body densities in $A = 2, 3, 4$ Nuclei (AV8')**

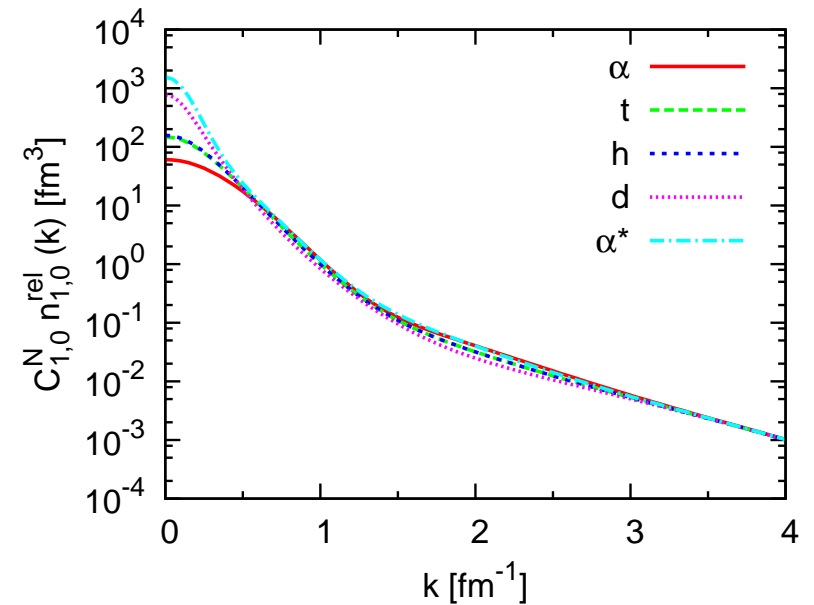
coordinate space

$S = 0, T = 1$



momentum space

$S = 0, T = 1$

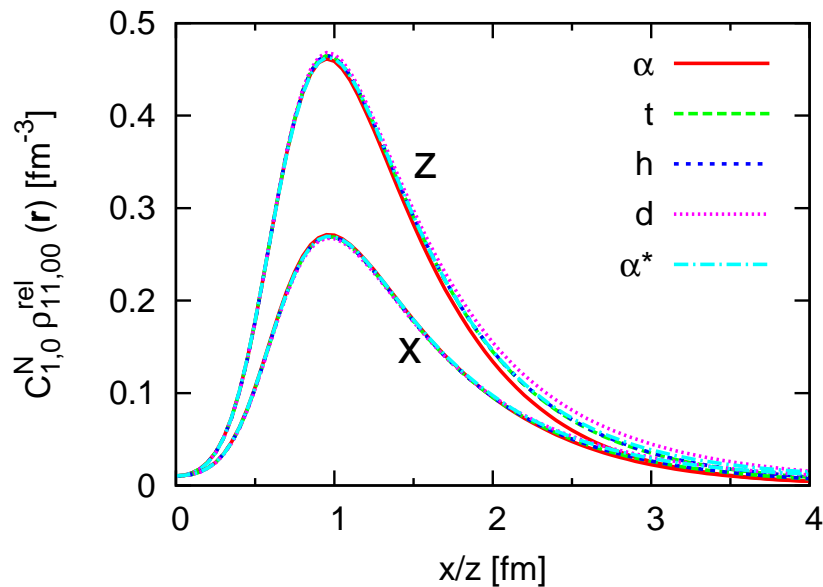


- normalize two-body density in coordinate space at $r=1.0$ fm
- normalized two-body densities in coordinate space are identical at short distances for all nuclei
- use the **same** normalization factor in momentum space – high momentum tails agree for all nuclei

- Short-range correlations
- **Two-body densities in $A = 2, 3, 4$ Nuclei (AV8')**

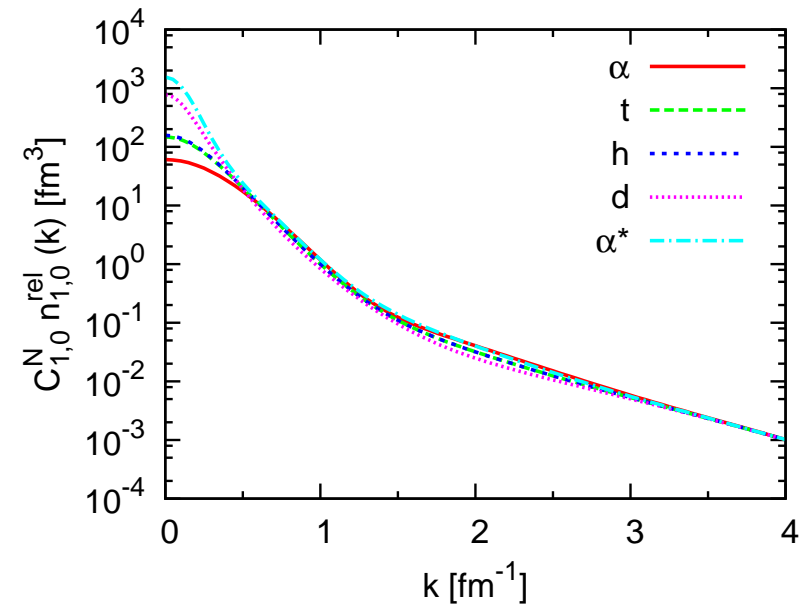
coordinate space

$S = 1, M_S = 1, T = 0$



momentum space

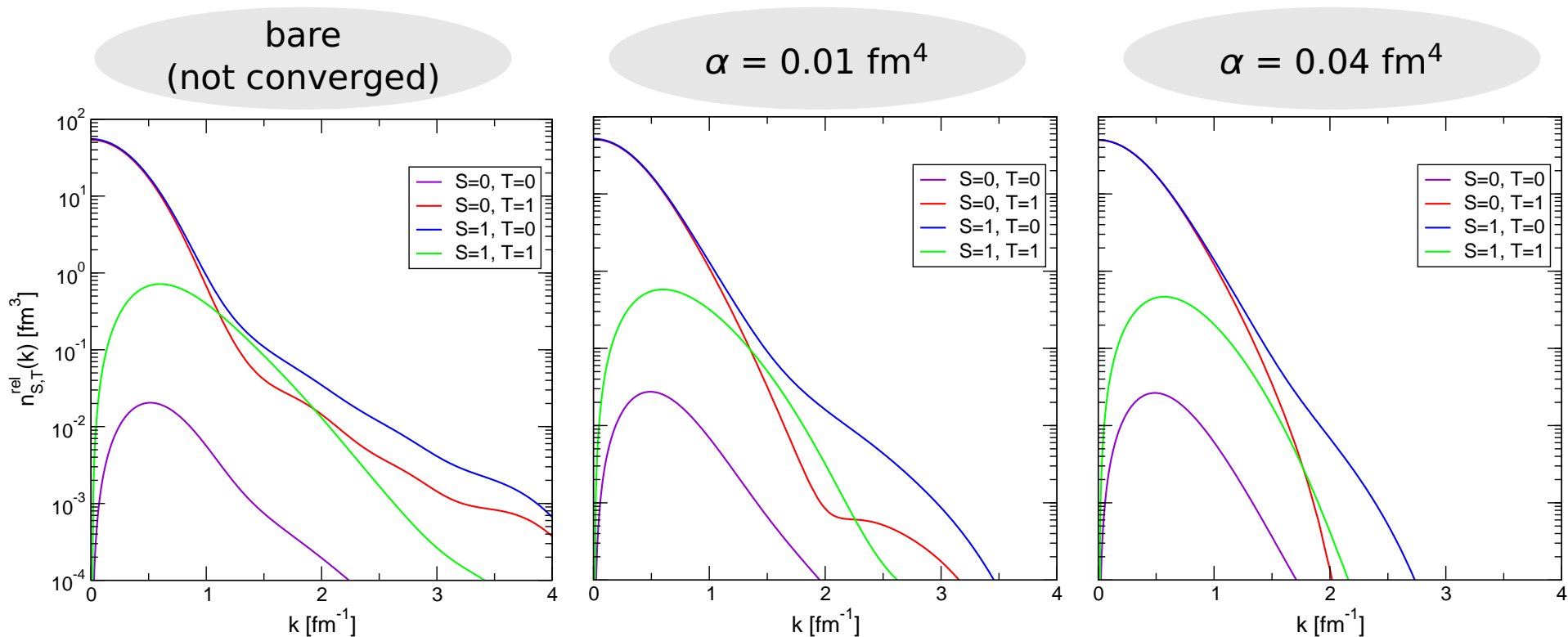
$S = 1, T = 0$



- normalize two-body density in coordinate space at $r=1.0$ fm averaged over all angles
- normalized two-body densities in coordinate space are identical at short distances for all nuclei
- use the **same** normalization factor in momentum space – high momentum tails agree for all nuclei

- Two-body densities

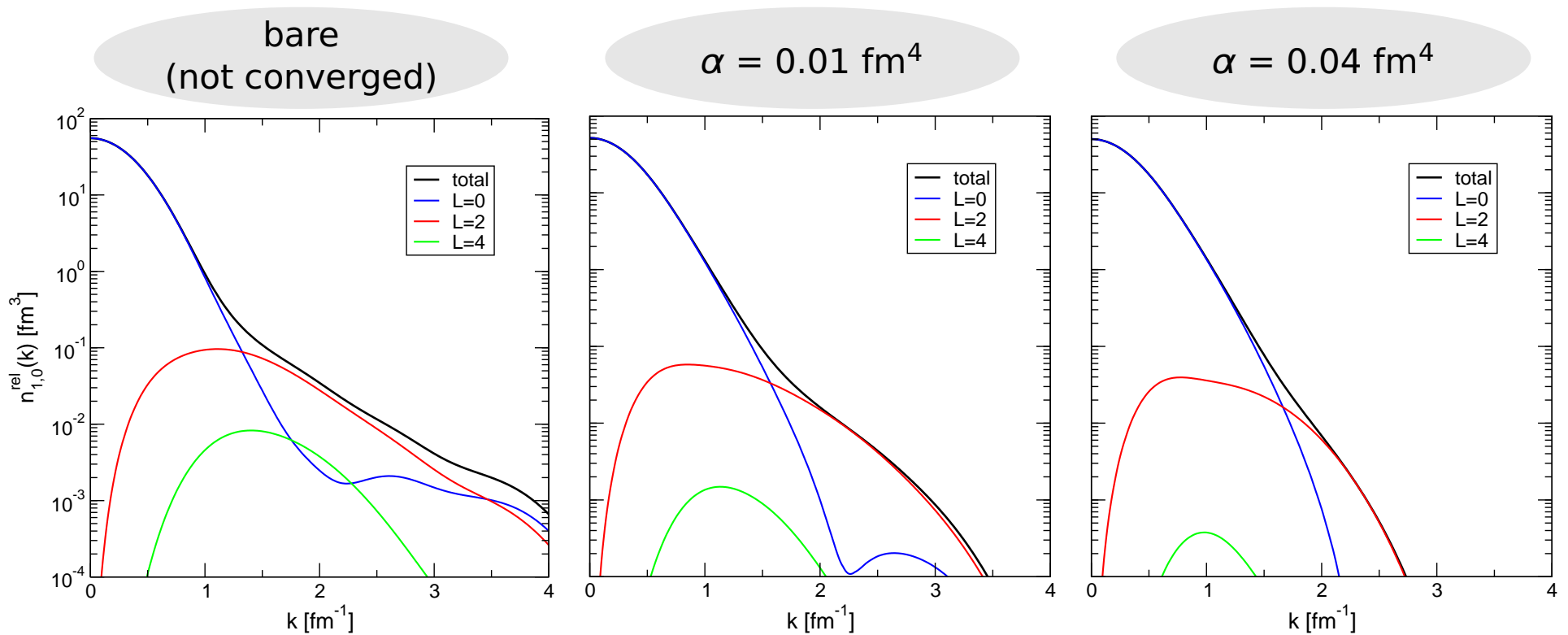
- ^4He : SRG evolved AV18, unevolved density operator



➔ NCSM calculations with $N_{\text{max}} = 16$

- bare interaction: 2.99 pairs in $S = 1, T = 0$ channel, 2.57 pairs in $S = 0, T = 1$ channel and 0.43 pairs in $S = 1, T = 1$ channel — tensor force induces three-body correlations
- high-momentum components reduced for evolved interactions
- number of $S = 1, T = 1$ pairs reduced for evolved interactions — weaker three-body correlations

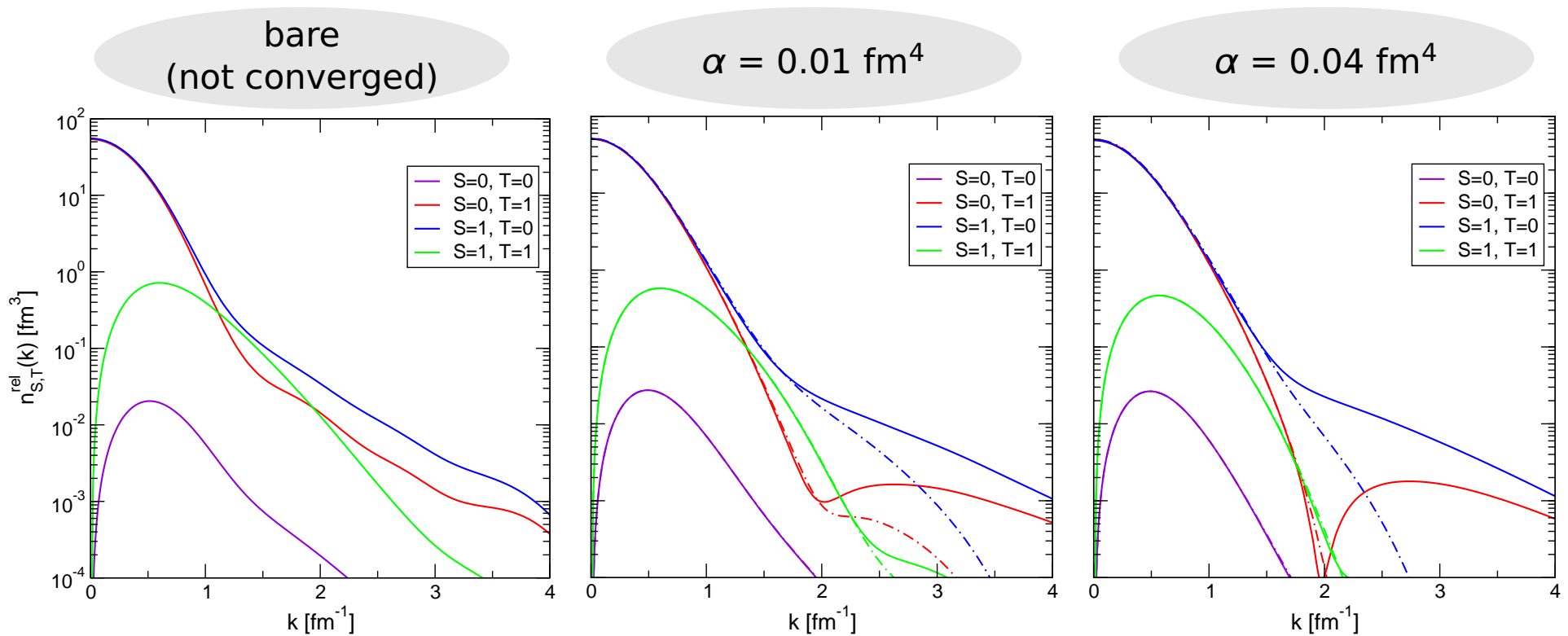
- Two-body densities $S = 1, T = 0$
- ^4He : SRG evolved AV18, unevolved density operator



- in the intermediate momentum region, momentum distribution dominated by D -wave contributions
- caused by tensor force, explains the enhancement of np -pairs versus pp -pairs above the Fermi momentum
- D -wave contributions reduced for evolved interactions – tensor force no longer connects to high momenta

- Two-body densities

- ^4He : SRG evolved AV18, evolved density operator



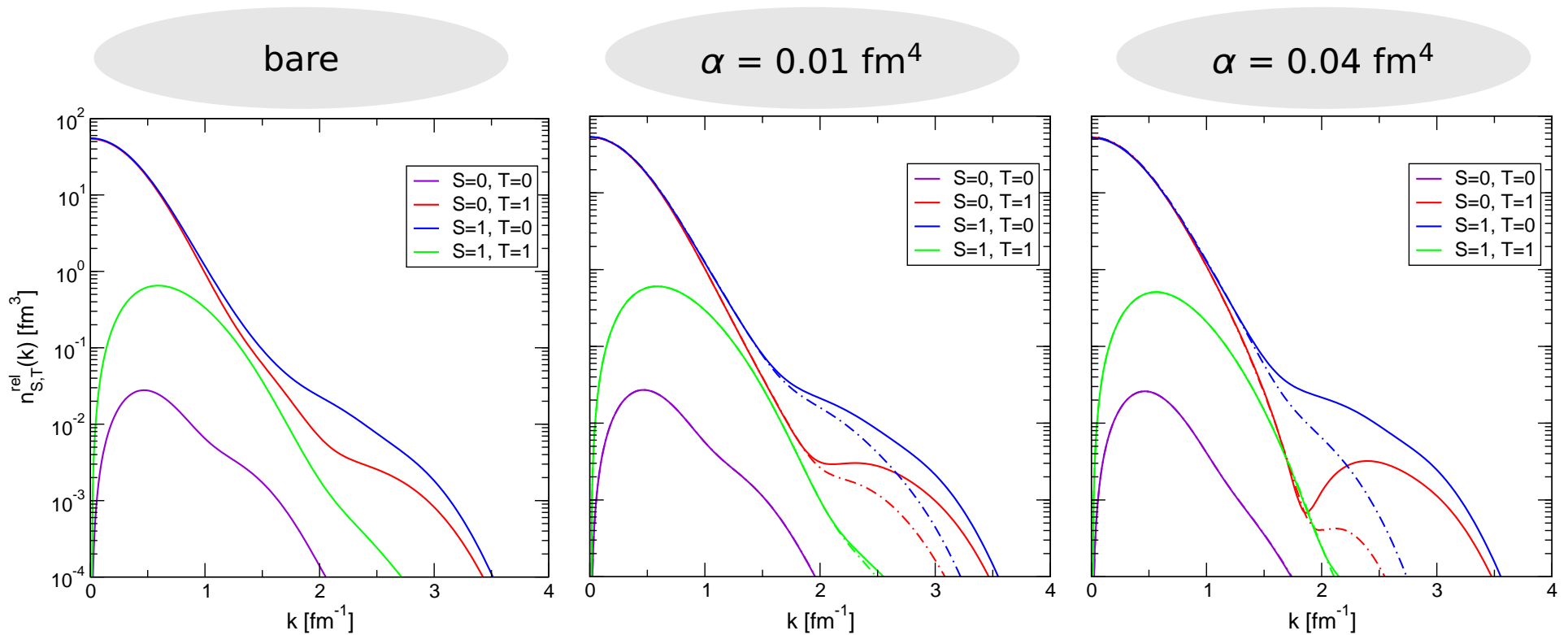
➔ use SRG transformed two-body density

- high-momentum components recovered

- significant differences for medium momenta — SRG done on two-body level for Hamiltonian and two-body density, three-body correlations important

- Two-body densities

- ^4He : SRG evolved N3LO, evolved density operator



- use SRG transformed two-body density

- high-momentum components recovered

- significant differences for medium momenta – SRG done on two-body level for Hamiltonian and two-body density

Unitary Correlation Operator Method



Short-range Correlations

Unitary Correlation Operator Method

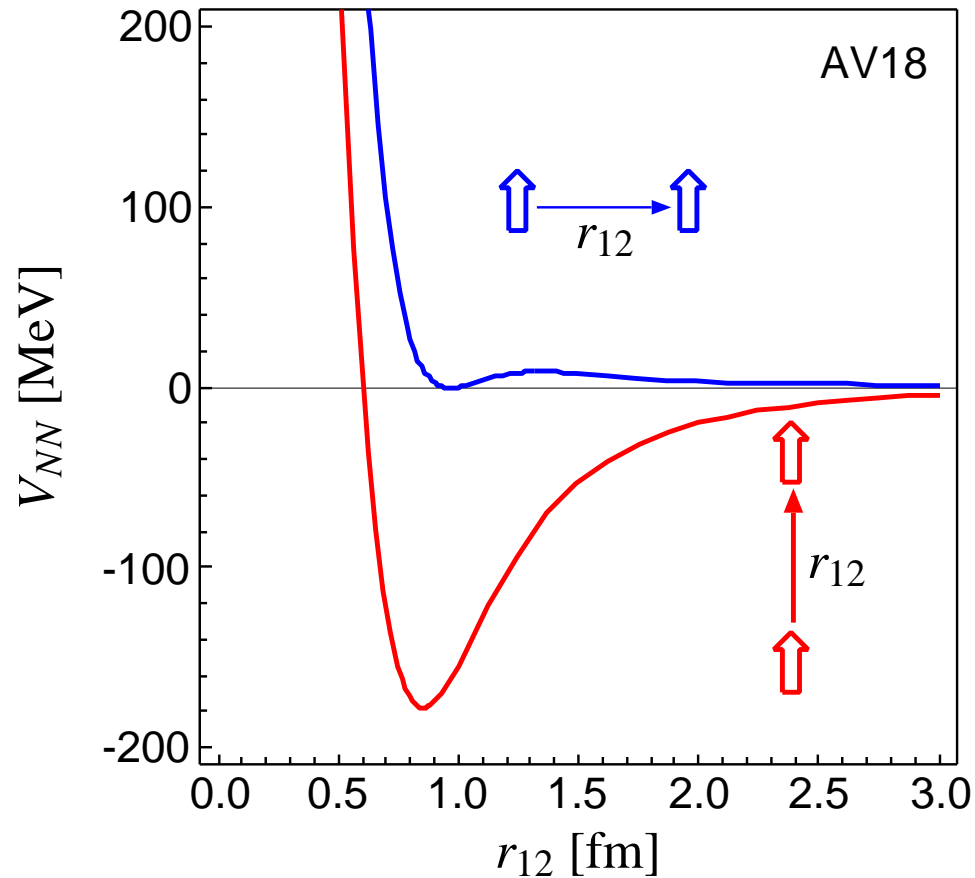
- Unitary Transformation
- Central and Tensor Correlations
- Interaction in Momentum Space
- Few-body Calculations

Unitary Correlation Operator Method

Nuclear Force

Argonne V18 (T=0)

spins aligned parallel or perpendicular to the relative distance vector



- strong repulsive core: nucleons can not get closer than ≈ 0.5 fm

➤ **central correlations**

- strong dependence on the orientation of the spins due to the tensor force

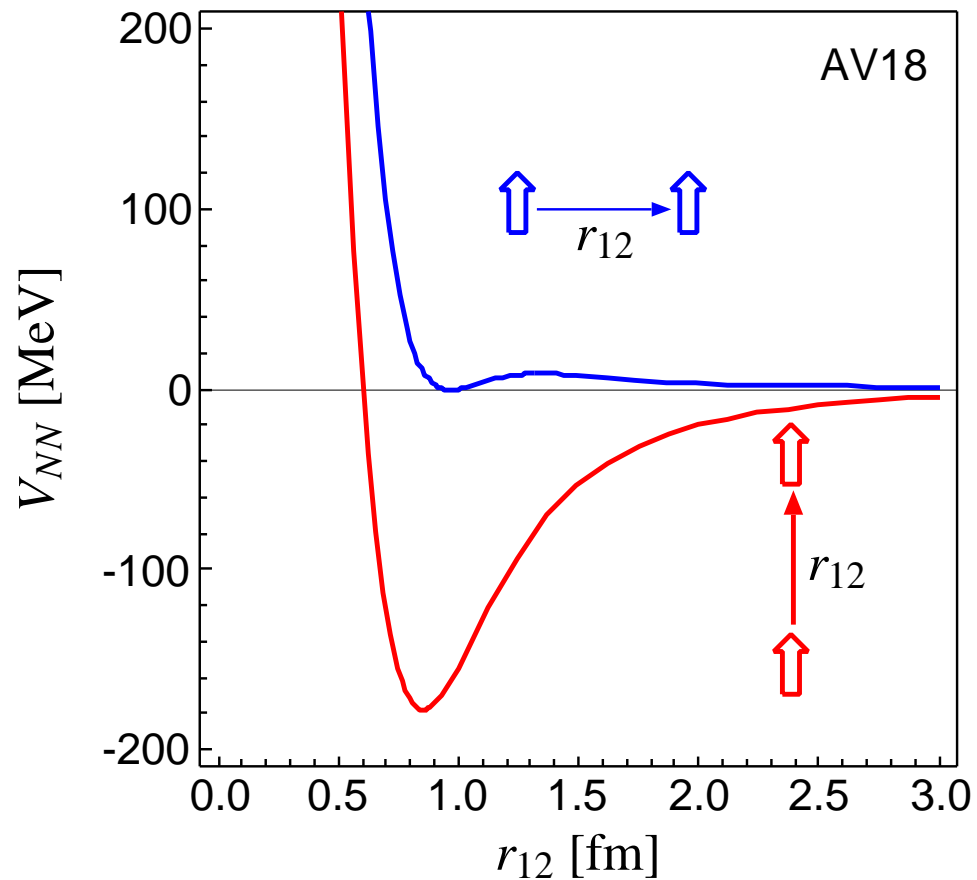
➤ **tensor correlations**

Unitary Correlation Operator Method

Nuclear Force

Argonne V18 (T=0)

spins aligned parallel or perpendicular to the relative distance vector



- strong repulsive core: nucleons can not get closer than ≈ 0.5 fm

➤ **central correlations**

- strong dependence on the orientation of the spins due to the tensor force

➤ **tensor correlations**

the nuclear force will induce **strong short-range correlations** in the nuclear wave function

Unitary Correlation Operator Method

Correlation Operator

- induce short-range (two-body) central and tensor correlations into the many-body state

$$\underline{\underline{C}} = \underline{\underline{C}}_{\Omega} \underline{\underline{C}}_r = \exp\left[-i \sum_{i<j} \underline{\underline{g}}_{\Omega,ij}\right] \exp\left[-i \sum_{i<j} \underline{\underline{g}}_{r,ij}\right] \quad , \quad \underline{\underline{C}}^{\dagger} \underline{\underline{C}} = \underline{\underline{1}}$$

- correlation operator should conserve the symmetries of the Hamiltonian and should be of finite-range, correlated interaction **phase shift equivalent** to bare interaction by construction

Correlated Operators

- correlated operators will have contributions in higher cluster orders

$$\underline{\underline{C}}^{\dagger} \underline{\underline{O}} \underline{\underline{C}} = \hat{\underline{\underline{O}}}^{[1]} + \hat{\underline{\underline{O}}}^{[2]} + \hat{\underline{\underline{O}}}^{[3]} + \dots$$

- two-body approximation: correlation range should be small compared to mean particle distance

Correlated Interaction

$$\underline{\underline{C}}^{\dagger} (\underline{\underline{T}} + \underline{\underline{V}}) \underline{\underline{C}} = \underline{\underline{T}} + \underline{\underline{V}}_{\text{UCOM}} + \underline{\underline{V}}_{\text{UCOM}}^{[3]} + \dots$$

- Central and Tensor Correlations

$$\tilde{C} = \tilde{C}_\Omega \tilde{C}_r$$

$$\mathbf{p} = \mathbf{p}_r + \mathbf{p}_\Omega$$

$$\mathbf{p}_r = \frac{1}{2} \left\{ \frac{\mathbf{r}}{r} \left(\frac{\mathbf{r}}{r} \mathbf{p} \right) + \left(\mathbf{p} \frac{\mathbf{r}}{r} \right) \frac{\mathbf{r}}{r} \right\}, \quad \mathbf{p}_\Omega = \frac{1}{2r} \left\{ \mathbf{l} \times \frac{\mathbf{r}}{r} - \frac{\mathbf{r}}{r} \times \mathbf{l} \right\}$$

Central and Tensor Correlations

$$\zeta = \zeta_{\Omega} \zeta_r$$

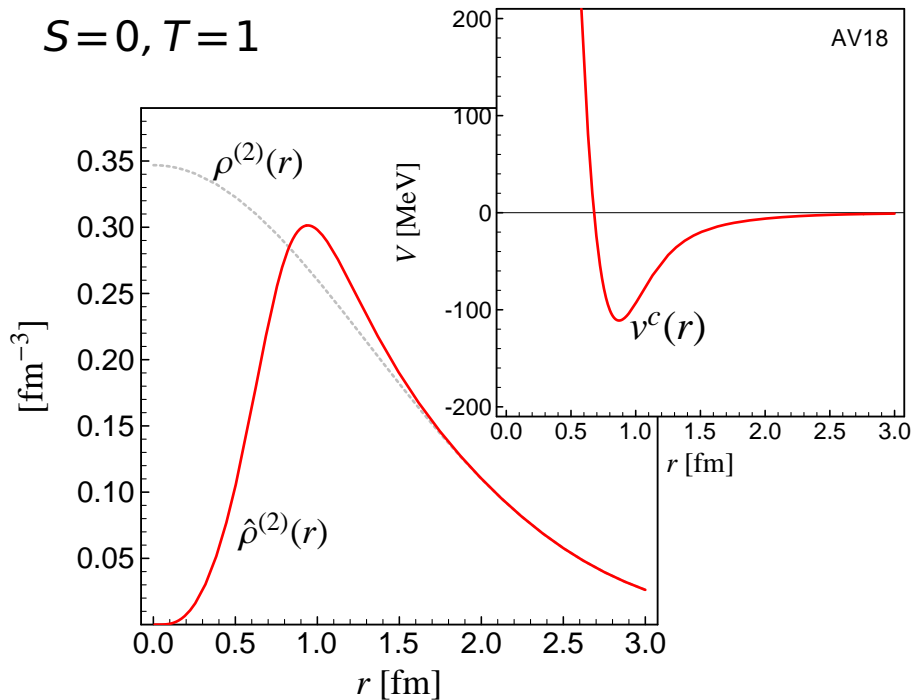
$$\mathbf{p} = \mathbf{p}_r + \mathbf{p}_{\Omega}$$

$$\mathbf{p}_r = \frac{1}{2} \left\{ \frac{\mathbf{r}}{r} (\mathbf{r} \cdot \mathbf{p}) + (\mathbf{p} \cdot \frac{\mathbf{r}}{r}) \frac{\mathbf{r}}{r} \right\}, \quad \mathbf{p}_{\Omega} = \frac{1}{2r} \left\{ \mathbf{l} \times \frac{\mathbf{r}}{r} - \frac{\mathbf{r}}{r} \times \mathbf{l} \right\}$$

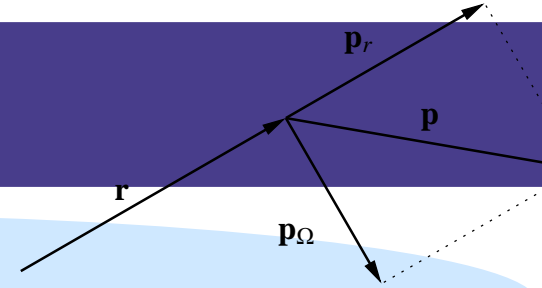
Central Correlations

$$\zeta_r = \exp \left\{ -\frac{i}{2} \{ p_r s(r) + s(r) p_r \} \right\}$$

→ probability density shifted out of the repulsive core



Central and Tensor Correlations



$$\zeta = \zeta_\Omega \zeta_r$$

$$\mathbf{p} = \mathbf{p}_r + \mathbf{p}_\Omega$$

$$\mathbf{p}_r = \frac{1}{2} \left\{ \frac{\mathbf{r}}{r} (\mathbf{r} \cdot \mathbf{p}) + (\mathbf{p} \cdot \frac{\mathbf{r}}{r}) \frac{\mathbf{r}}{r} \right\}, \quad \mathbf{p}_\Omega = \frac{1}{2r} \{ \mathbf{l} \times \frac{\mathbf{r}}{r} - \frac{\mathbf{r}}{r} \times \mathbf{l} \}$$

Central Correlations

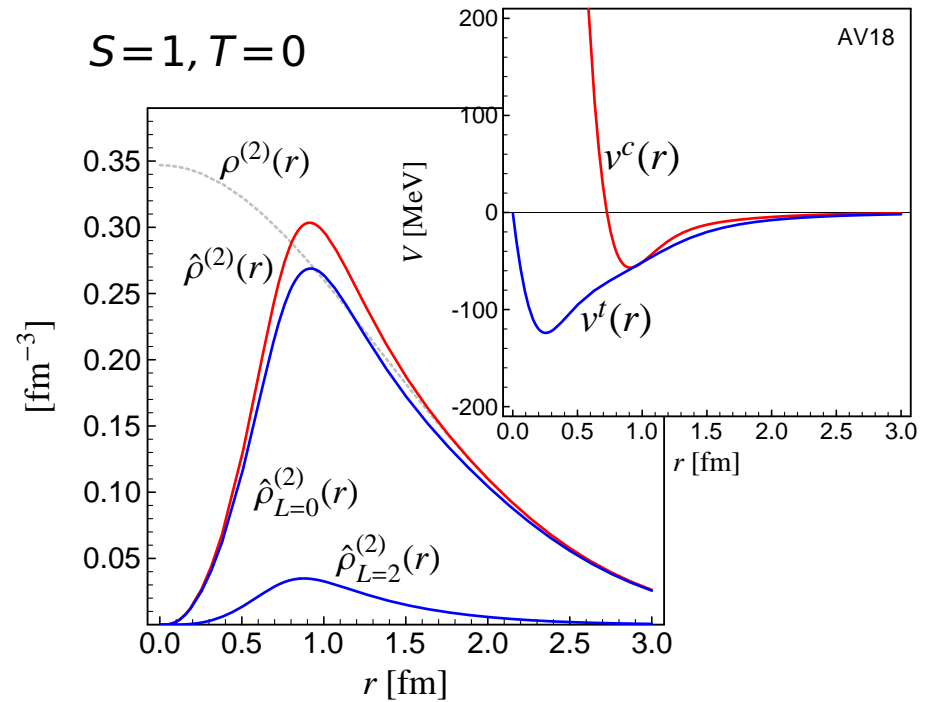
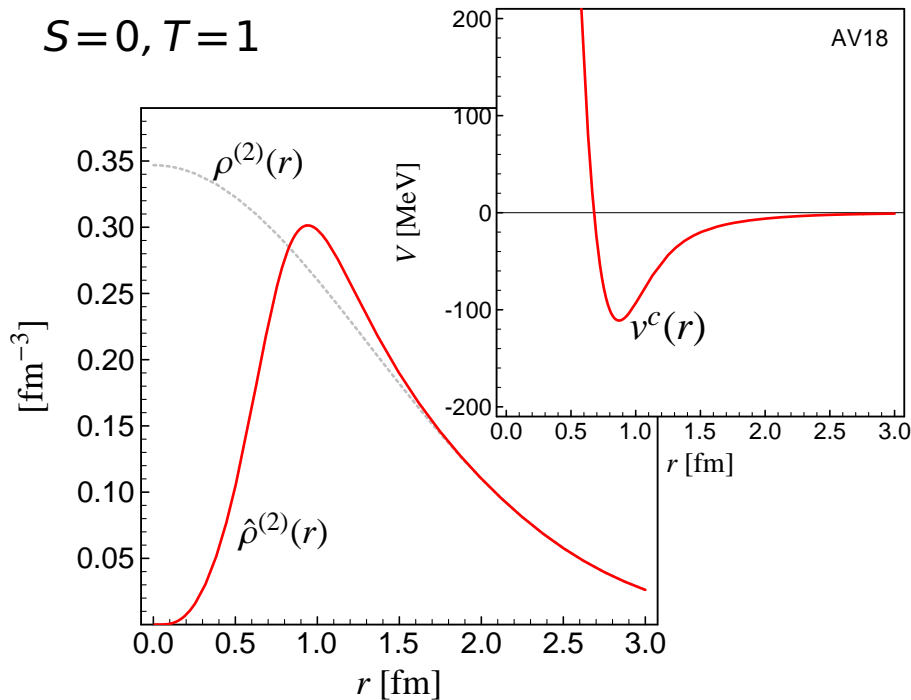
$$\zeta_r = \exp \left\{ -\frac{i}{2} \{ p_r s(r) + s(r) p_r \} \right\}$$

→ probability density shifted out of the repulsive core

Tensor Correlations

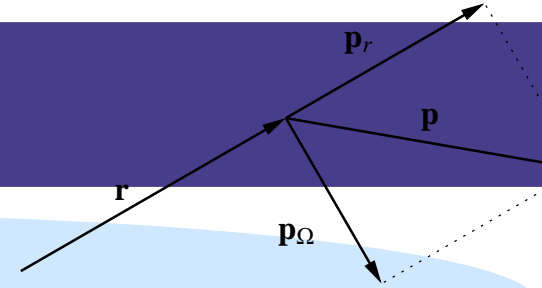
$$\zeta_\Omega = \exp \left\{ -i\theta(r) \left\{ \frac{3}{2} (\boldsymbol{\sigma}_1 \cdot \mathbf{p}_\Omega) (\boldsymbol{\sigma}_2 \cdot \mathbf{r}) + \frac{3}{2} (\boldsymbol{\sigma}_1 \cdot \mathbf{r}) (\boldsymbol{\sigma}_2 \cdot \mathbf{p}_\Omega) \right\} \right\}$$

→ tensor force admixes other angular momenta



UCOM

Central and Tensor Correlations



$$\zeta = \zeta_\Omega \zeta_r$$

$$\mathbf{p} = \mathbf{p}_r + \mathbf{p}_\Omega$$

$$\mathbf{p}_r = \frac{1}{2} \left\{ \frac{\mathbf{r}}{r} (\mathbf{r} \cdot \mathbf{p}) + (\mathbf{p} \cdot \frac{\mathbf{r}}{r}) \frac{\mathbf{r}}{r} \right\}, \quad \mathbf{p}_\Omega = \frac{1}{2r} \left\{ \mathbf{l} \times \frac{\mathbf{r}}{r} - \frac{\mathbf{r}}{r} \times \mathbf{l} \right\}$$

Central Correlations

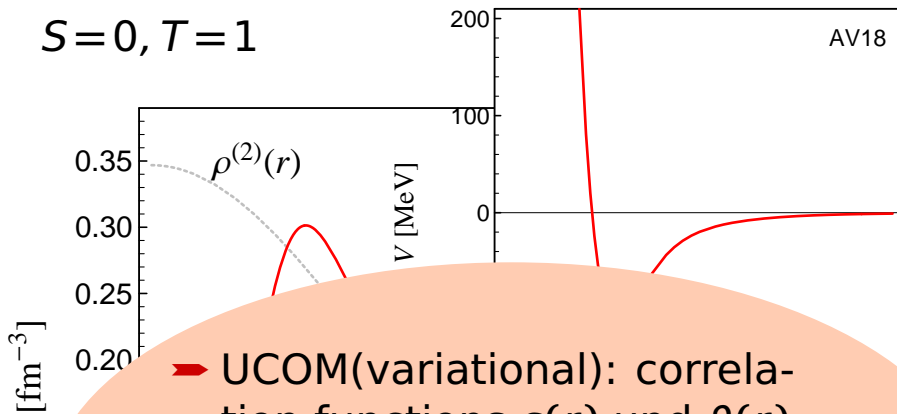
$$\zeta_r = \exp \left\{ -\frac{i}{2} \{ p_r s(r) + s(r) p_r \} \right\}$$

→ probability density shifted out of the repulsive core

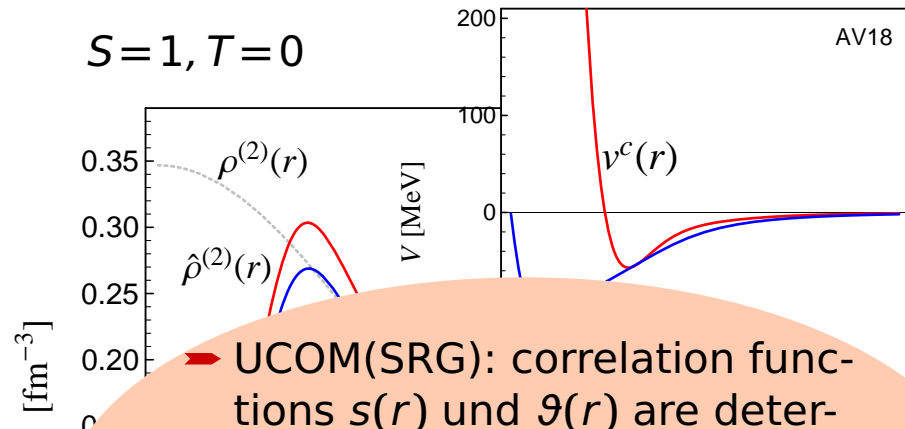
Tensor Correlations

$$\zeta_\Omega = \exp \left\{ -i\vartheta(r) \left\{ \frac{3}{2} (\boldsymbol{\sigma}_1 \cdot \mathbf{p}_\Omega) (\boldsymbol{\sigma}_2 \cdot \mathbf{r}) + \frac{3}{2} (\boldsymbol{\sigma}_1 \cdot \mathbf{r}) (\boldsymbol{\sigma}_2 \cdot \mathbf{p}_\Omega) \right\} \right\}$$

→ tensor force admixes other angular momenta



→ UCOM(variational): correlation functions $s(r)$ and $\vartheta(r)$ are determined by **variation** of the energy in the **two-body system** for each S, T channel

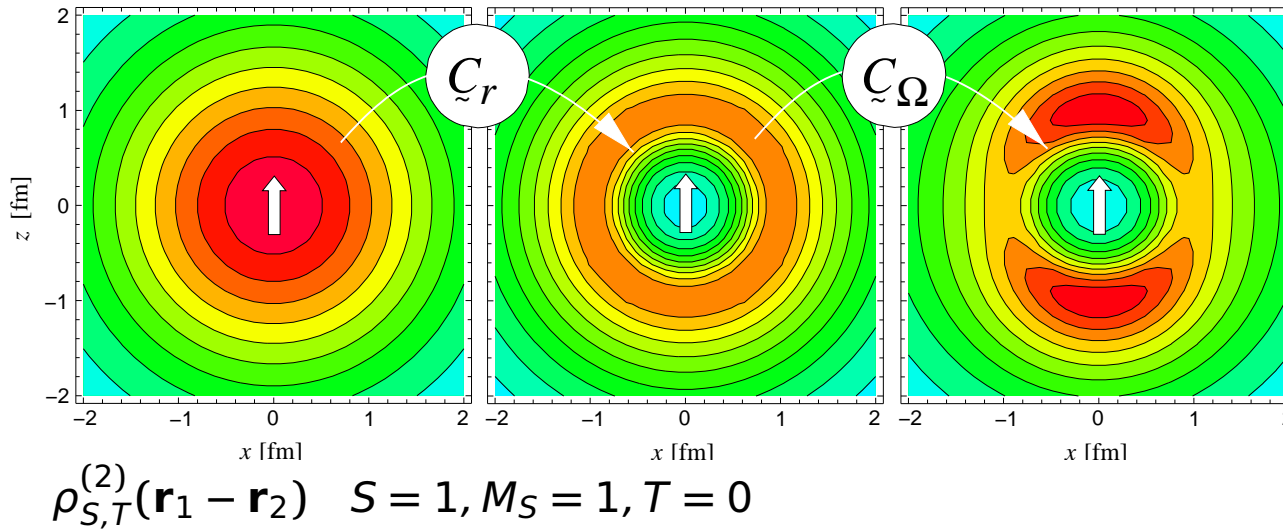


→ UCOM(SRG): correlation functions $s(r)$ and $\vartheta(r)$ are determined from **mapping wave functions** obtained with **bare interaction** to wave functions obtained with **SRG interaction**

Unitary Correlation Operator Method

Correlations and Energies

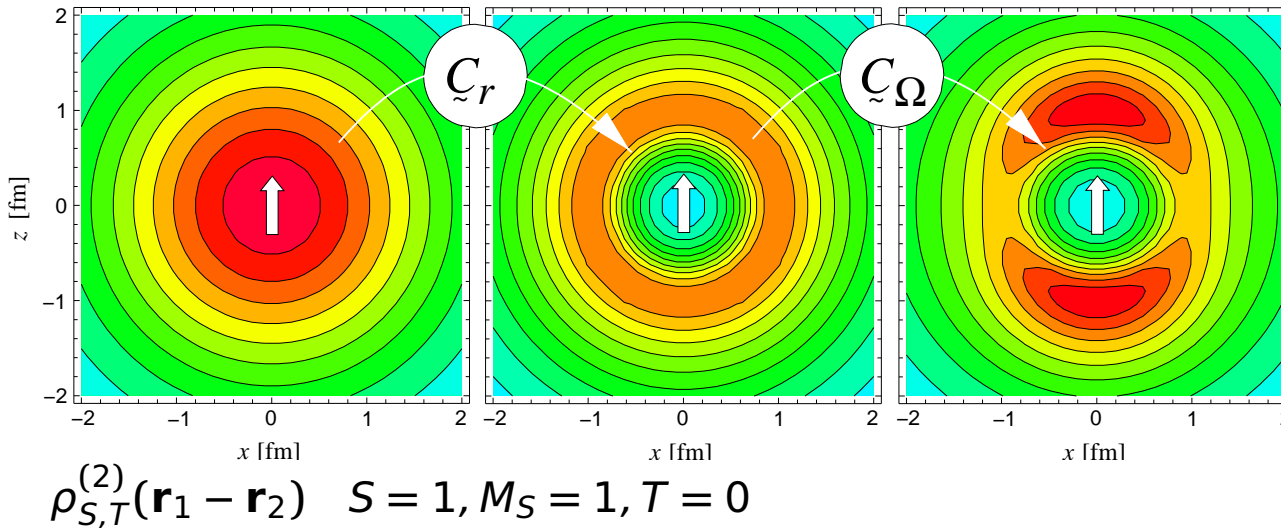
two-body densities



central correlator \tilde{C}_r
 shifts density out of
 the repulsive core
tensor correlator \tilde{C}_Ω
 aligns density with spin
 orientation

Unitary Correlation Operator Method Correlations and Energies

two-body densities

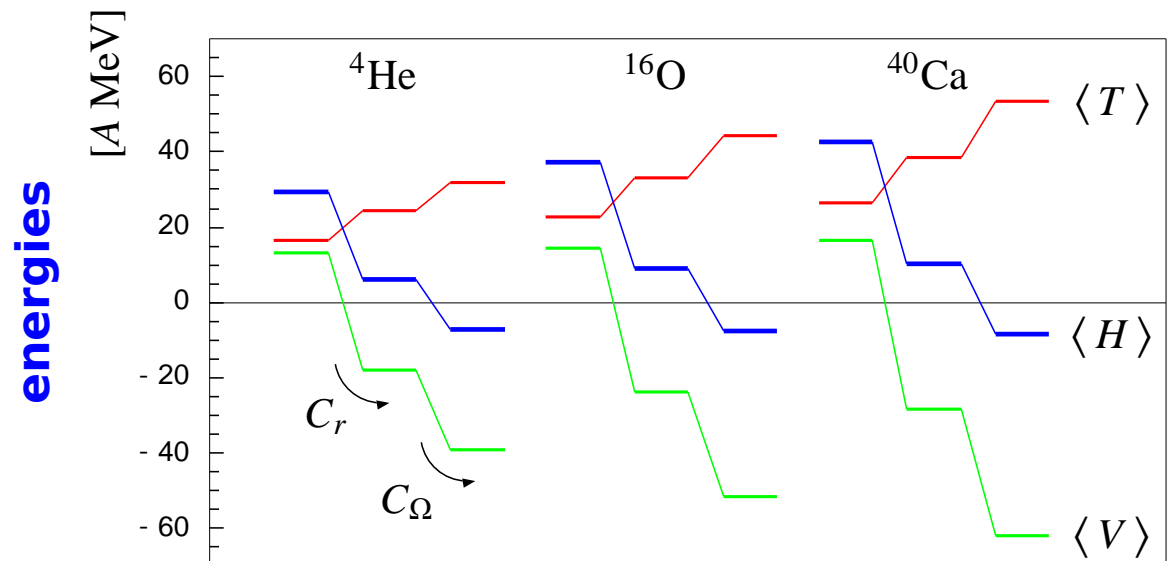


central correlator \tilde{C}_r
shifts density out of
the repulsive core

tensor correlator \tilde{C}_Ω
aligns density with spin
orientation

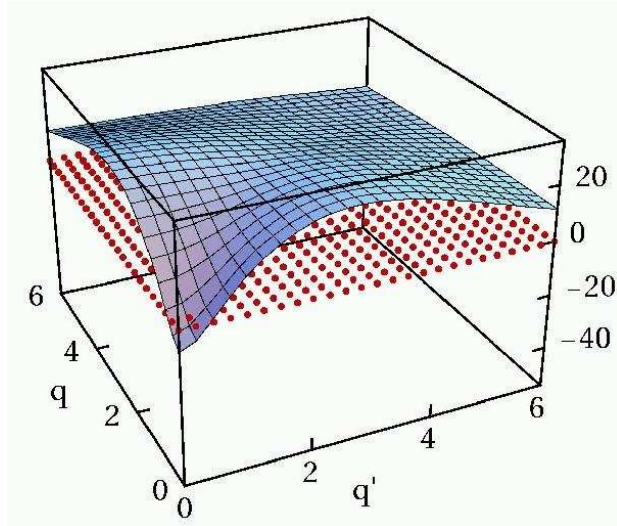
both central
and tensor
correlations are
essential for
binding

$0\hbar\omega$ Harmonic Oscillator



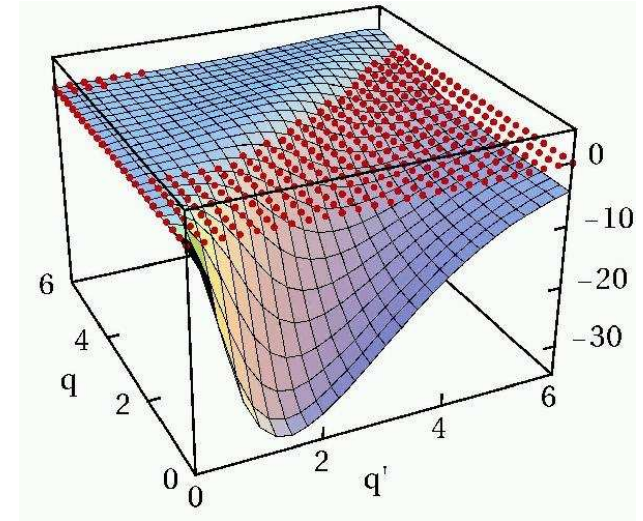
- Unitary Correlation Operator Method
- **Correlated Interaction in Momentum Space**

3S_1 bare



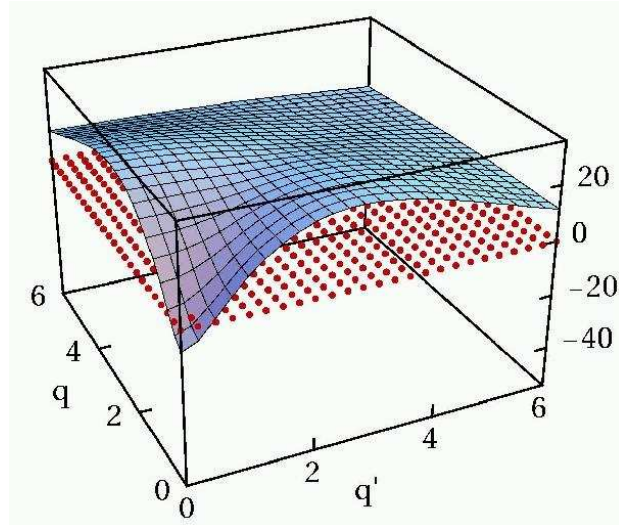
bare interaction has **strong off-diagonal** matrix elements connecting to high momenta

${}^3S_1 - {}^3D_1$ bare



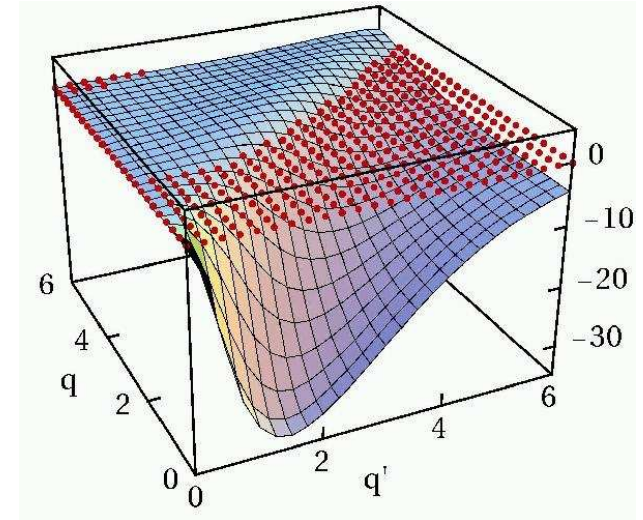
- Unitary Correlation Operator Method
- **Correlated Interaction in Momentum Space**

3S_1 bare



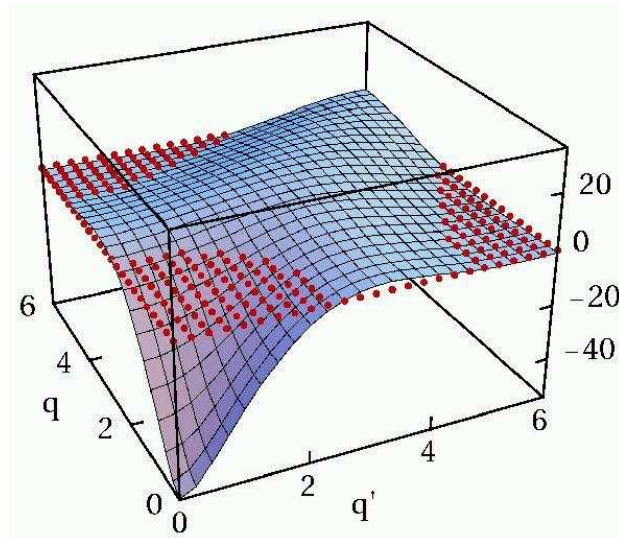
bare interaction has **strong off-diagonal** matrix elements connecting to high momenta

${}^3S_1 - {}^3D_1$ bare



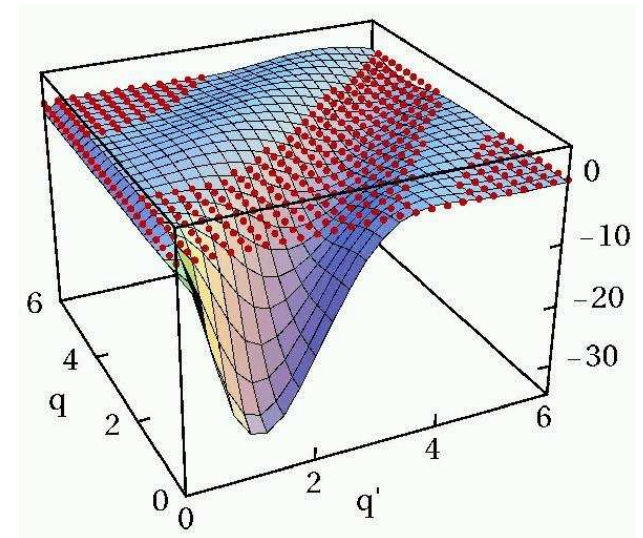
correlated interaction is **more attractive** at low momenta

3S_1 correlated



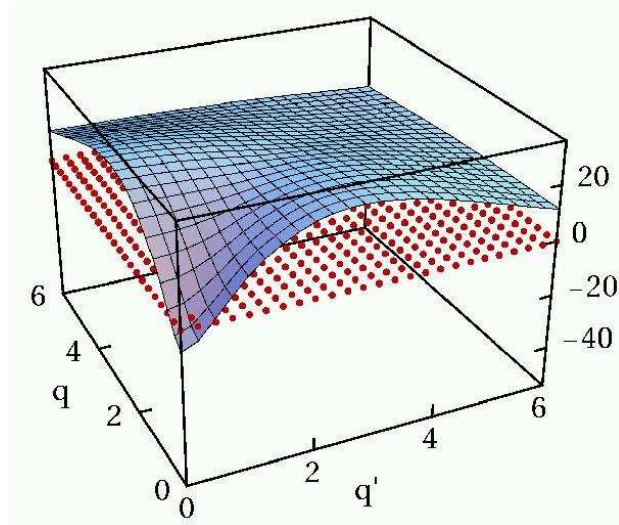
off-diagonal matrix elements connecting low- and high- momentum states are **strongly reduced**

${}^3S_1 - {}^3D_1$ correlated



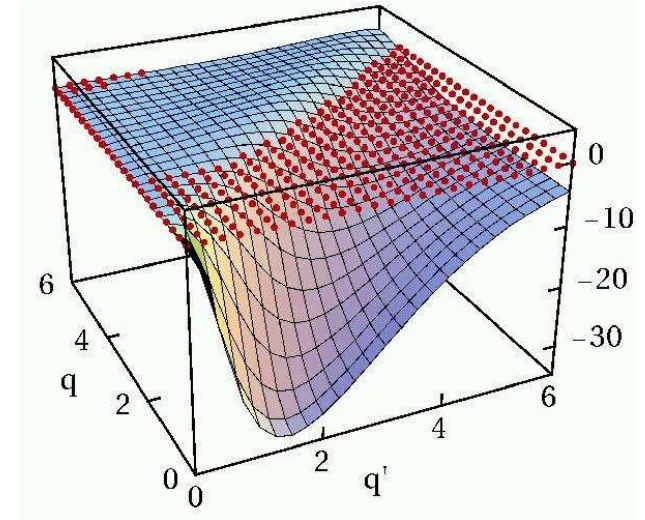
- Unitary Correlation Operator Method
- **Correlated Interaction in Momentum Space**

3S_1 bare



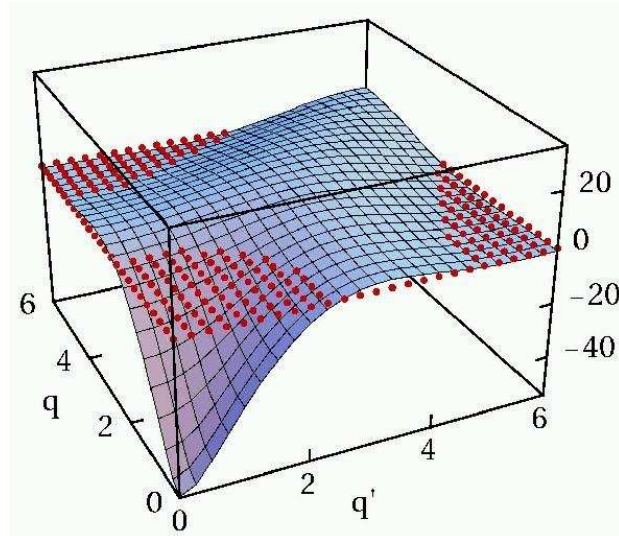
bare interaction has **strong off-diagonal** matrix elements connecting to high momenta

${}^3S_1 - {}^3D_1$ bare



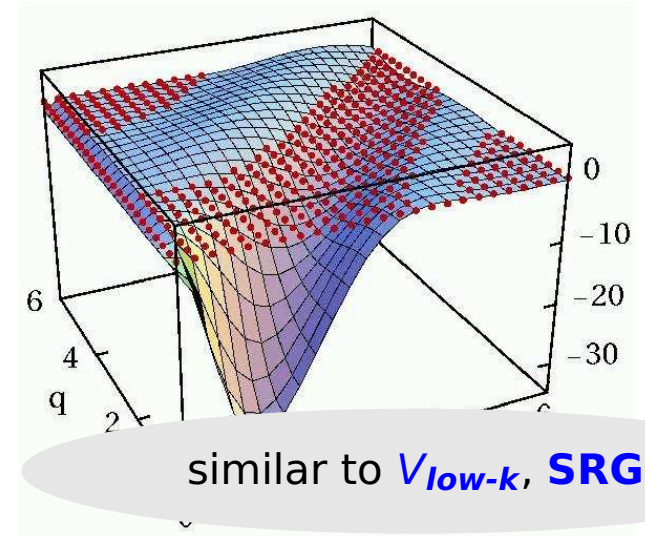
correlated interaction is **more attractive** at low momenta

3S_1 correlated

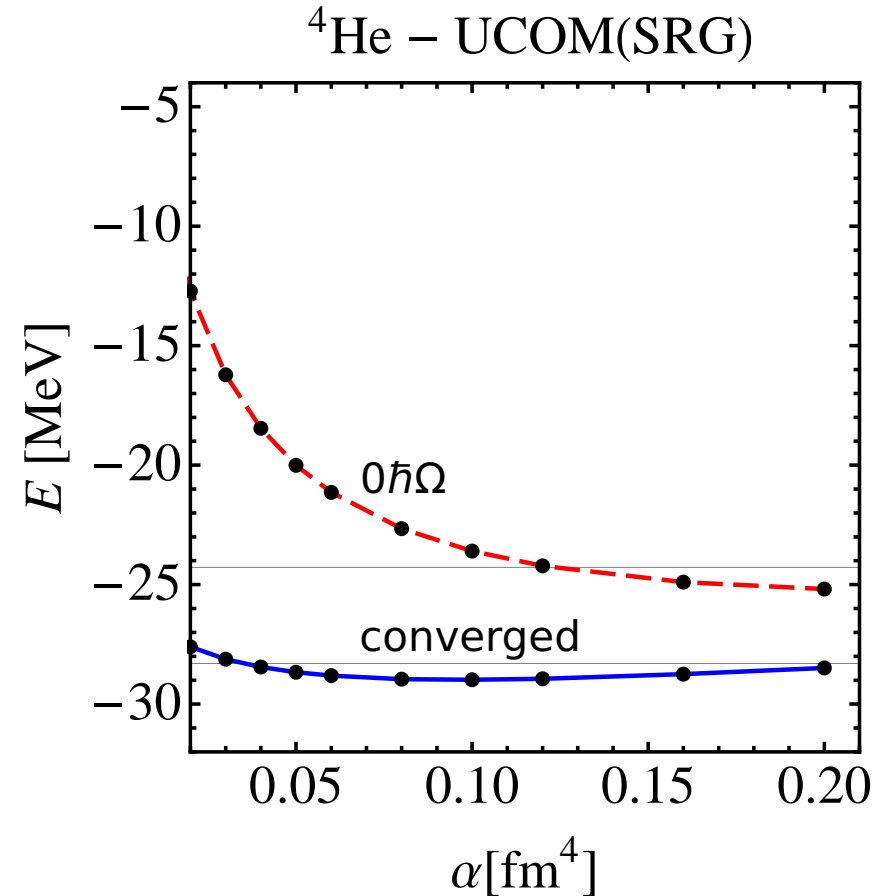
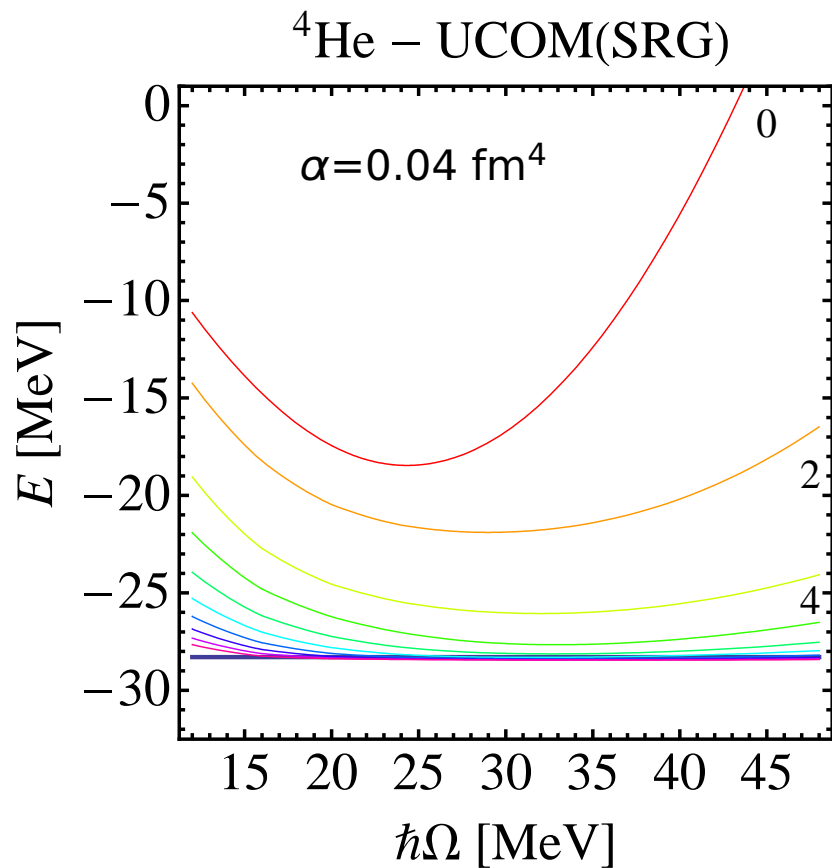


off-diagonal matrix elements connecting low- and high- momentum states are **strongly reduced**

${}^3S_1 - {}^3D_1$ correlated



similar to V_{low-k} , **SRG**



- convergence much improved compared to bare interaction
- effective interaction – in two-body approximation – converges to different energy than bare interaction
- transformed interaction can be tuned to obtain simultaneously (almost) exact ${}^3\text{He}$ and ${}^4\text{He}$ binding energies

Fermionic

Slater determinant

$$|Q\rangle = \mathcal{A}\left(|q_1\rangle \otimes \cdots \otimes |q_A\rangle\right)$$

- antisymmetrized A -body state

Fermionic

Slater determinant

$$|Q\rangle = \mathcal{A}\left(|q_1\rangle \otimes \cdots \otimes |q_A\rangle\right)$$

- antisymmetrized A -body state

Molecular

single-particle states

$$\langle \mathbf{x} | q \rangle = \sum_i c_i \exp\left\{-\frac{(\mathbf{x} - \mathbf{b}_i)^2}{2a_i}\right\} \otimes |\chi_i^\uparrow, \chi_i^\downarrow\rangle \otimes |\xi\rangle$$

- Gaussian wave-packets in phase-space (complex parameter \mathbf{b}_i encodes mean position and mean momentum), spin is free, isospin is fixed
- width a_i is an independent variational parameter for each wave packet
- use one or two wave packets for each single particle state

Fermionic

Slater determinant

$$|Q\rangle = \mathcal{A}\left(|q_1\rangle \otimes \cdots \otimes |q_A\rangle\right)$$

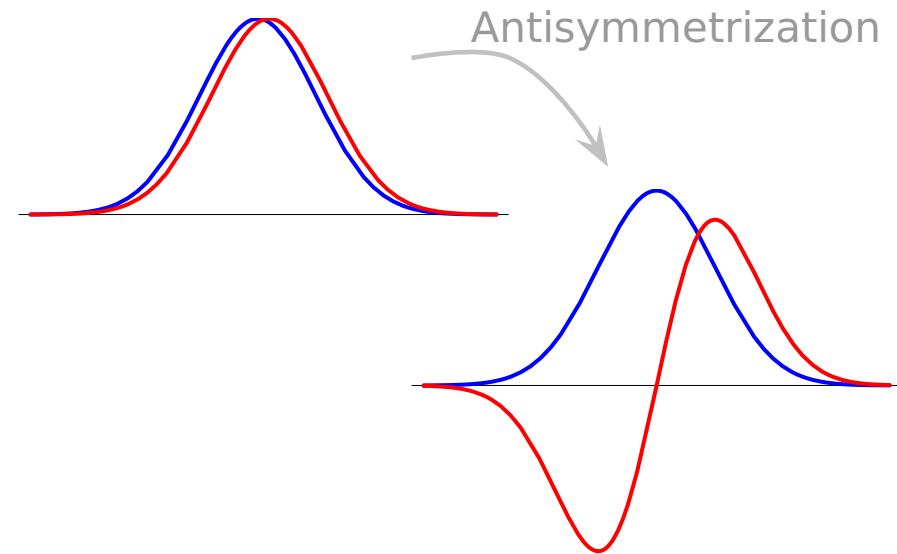
- antisymmetrized A-body state

Molecular

single-particle states

$$\langle \mathbf{x} | q \rangle = \sum_i c_i \exp\left\{-\frac{(\mathbf{x} - \mathbf{b}_i)^2}{2a_i}\right\} \otimes |\chi_i^\uparrow, \chi_i^\downarrow\rangle \otimes |\xi\rangle$$

- Gaussian wave-packets in phase-space (complex parameter \mathbf{b}_i encodes mean position and mean momentum), spin is free, isospin is fixed
- width a_i is an independent variational parameter for each wave packet
- use one or two wave packets for each single particle state



Fermionic Molecular Dynamics

Fermionic

Slater determinant

$$|Q\rangle = \mathcal{A}\left(|q_1\rangle \otimes \cdots \otimes |q_A\rangle\right)$$

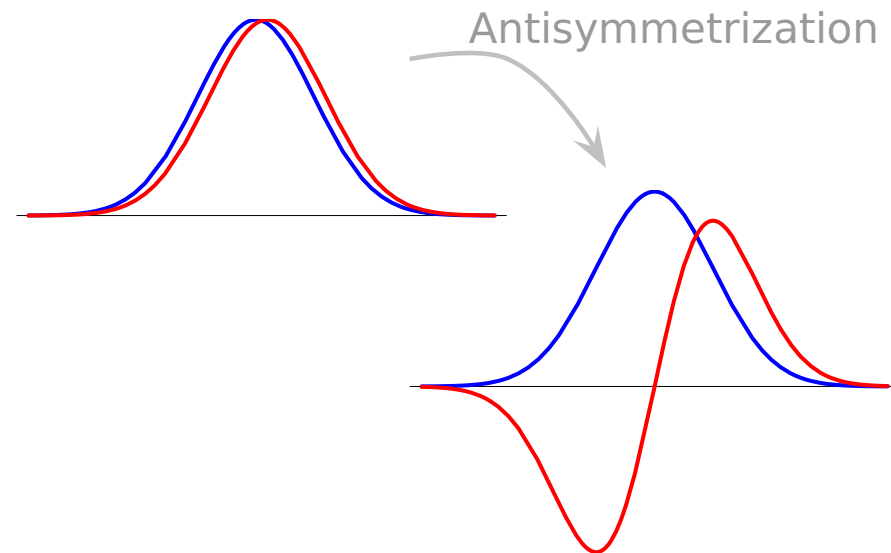
- antisymmetrized A-body state

Molecular

single-particle states

$$\langle \mathbf{x} | q \rangle = \sum_i c_i \exp\left\{-\frac{(\mathbf{x} - \mathbf{b}_i)^2}{2a_i}\right\} \otimes |\chi_i^\uparrow, \chi_i^\downarrow\rangle \otimes |\xi\rangle$$

- Gaussian wave-packets in phase-space (complex parameter \mathbf{b}_i encodes mean position and mean momentum), spin is free, isospin is fixed
- width a_i is an independent variational parameter for each wave packet
- use one or two wave packets for each single particle state



see also
**Antisymmetrized
 Molecular Dynamics**
 Horiuchi, Kanada-En'yo,
 Kimura, ...

Interaction Matrix Elements

(One-body) Kinetic Energy

$$\langle q_k | \tilde{T} | q_l \rangle = \langle a_k \mathbf{b}_k | \tilde{T} | a_l \mathbf{b}_l \rangle \langle \chi_k | \chi_l \rangle \langle \xi_k | \xi_l \rangle$$

$$\langle a_k \mathbf{b}_k | \tilde{T} | a_l \mathbf{b}_l \rangle = \frac{1}{2m} \left(\frac{3}{a_k^* + a_l} - \frac{(\mathbf{b}_k^* - \mathbf{b}_l)^2}{(a_k^* + a_l)^2} \right) R_{kl}$$

(Two-body) Potential

→ fit radial dependencies by (a sum of) Gaussians

$$G(\mathbf{x}_1 - \mathbf{x}_2) = \exp \left\{ -\frac{(\mathbf{x}_1 - \mathbf{x}_2)^2}{2K} \right\}$$

→ Gaussian integrals

$$\langle a_k \mathbf{b}_k, a_l \mathbf{b}_l | \tilde{G} | a_m \mathbf{b}_m, a_n \mathbf{b}_n \rangle = R_{km} R_{ln} \left(\frac{K}{\alpha_{klmn} + K} \right)^{3/2} \exp \left\{ -\frac{\rho_{klmn}^2}{2(\alpha_{klmn} + K)} \right\}$$

→ analytical expressions for matrix elements

$$\alpha_{klmn} = \frac{a_k^* a_m}{a_k^* + a_m} + \frac{a_l^* a_n}{a_l^* + a_n}$$

$$\rho_{klmn} = \frac{a_m \mathbf{b}_k^* + a_k^* \mathbf{b}_m}{a_k^* + a_m} - \frac{a_n \mathbf{b}_l^* + a_l^* \mathbf{b}_n}{a_l^* + a_n}$$

$$R_{km} = \langle a_k \mathbf{b}_k | a_m \mathbf{b}_m \rangle$$

Operator Representation of V_{UCOM}

$$\tilde{\zeta}^\dagger (\tilde{T} + \tilde{V}) \tilde{\zeta} = \tilde{T}$$

$$+ \sum_{ST} \hat{V}_c^{ST}(r) + \frac{1}{2} (p_r^2 \hat{V}_{p^2}^{ST}(r) + \hat{V}_{p^2}^{ST}(r) p_r^2) + \hat{V}_{l^2}^{ST}(r) \mathbf{l}^2$$

one-body kinetic energy

central potentials

$$+ \sum_T \hat{V}_{ls}^T(r) \mathbf{l} \cdot \mathbf{s} + \hat{V}_{l^2ls}^T(r) \mathbf{l}^2 \mathbf{l} \cdot \mathbf{s}$$

spin-orbit potentials

$$+ \sum_T \hat{V}_t^T(r) \tilde{\zeta}_{12}(\mathbf{r}, \mathbf{r}) + \hat{V}_{trp_\Omega}^T(r) p_r \tilde{\zeta}_{12}(\mathbf{r}, \mathbf{p}_\Omega) + \hat{V}_{tll}^T(r) \tilde{\zeta}_{12}(\mathbf{l}, \mathbf{l}) +$$

$$\hat{V}_{tp_\Omega p_\Omega}^T(r) \tilde{\zeta}_{12}(\mathbf{p}_\Omega, \mathbf{p}_\Omega) + \hat{V}_{l^2tp_\Omega p_\Omega}^T(r) \mathbf{l}^2 \tilde{\zeta}_{12}(\mathbf{p}_\Omega, \mathbf{p}_\Omega)$$

tensor potentials

bulk of tensor force mapped onto central part
of correlated interaction

tensor correlations also change the spin-orbit
part of the interaction

Projection After Variation (PAV)

- mean-field may break symmetries of Hamiltonian
- restore inversion, translational and rotational symmetry by projection on parity, linear and angular momentum

$$\tilde{P}^\pi = \frac{1}{2}(1 + \pi\tilde{\Pi})$$

$$\tilde{P}_{MK}^J = \frac{2J + 1}{8\pi^2} \int d^3\Omega D_{MK}^{J*}(\Omega) \tilde{R}(\Omega)$$

$$\tilde{P}^{\mathbf{P}} = \frac{1}{(2\pi)^3} \int d^3\mathbf{X} \exp\{-i(\tilde{\mathbf{P}} - \mathbf{P}) \cdot \mathbf{X}\}$$

Projection After Variation (PAV)

- mean-field may break symmetries of Hamiltonian
- restore inversion, translational and rotational symmetry by projection on parity, linear and angular momentum

$$\tilde{P}^{\pi} = \frac{1}{2}(1 + \pi\tilde{\Pi})$$

$$\tilde{P}_{MK}^J = \frac{2J+1}{8\pi^2} \int d^3\Omega D_{MK}^{J*}(\Omega) \tilde{R}(\Omega)$$

Variation After Projection (VAP)

- effect of projection can be large
- full **Variation after Angular Momentum and Parity Projection** (VAP) for light nuclei
- perform VAP in GCM sense by applying **constraints** on **radius**, **dipole moment**, **quadrupole moment** or **octupole moment** and minimizing the energy in the projected energy surface for heavier nuclei

$$\tilde{P}^{\mathbf{P}} = \frac{1}{(2\pi)^3} \int d^3\mathbf{X} \exp\{-i(\tilde{\mathbf{P}} - \mathbf{P}) \cdot \mathbf{X}\}$$

PAV, VAP and Multiconfiguration

Projection After Variation (PAV)

- mean-field may break symmetries of Hamiltonian
- restore inversion, translational and rotational symmetry by projection on parity, linear and angular momentum

$$\tilde{P}^\pi = \frac{1}{2}(1 + \pi\Pi)$$

$$\tilde{P}_{MK}^J = \frac{2J+1}{8\pi^2} \int d^3\Omega D_{MK}^{J*}(\Omega) \tilde{P}(\Omega)$$

Variation After Projection (VAP)

- effect of projection can be large
- full **Variation after Angular Momentum and Parity Projection** (VAP) for light nuclei
- perform VAP in GCM sense by applying **constraints** on **radius**, **dipole moment**, **quadrupole moment** or **octupole moment** and minimizing the energy in the projected energy surface for heavier nuclei

$$\tilde{P}^{\mathbf{P}} = \frac{1}{(2\pi)^3} \int d^3\mathbf{X} \exp\{-i(\tilde{\mathbf{P}} - \mathbf{P}) \cdot \mathbf{X}\}$$

Multiconfiguration Calculations

- **diagonalize** Hamiltonian in a set of projected intrinsic states

$$\left\{ |Q^{(a)}\rangle, \quad a = 1, \dots, N \right\}$$

$$\sum_{K'b} \langle Q^{(a)} | \tilde{H} \tilde{P}_{KK'}^{J\pi} \tilde{P}^{\mathbf{P}=0} | Q^{(b)} \rangle \cdot c_{K'b}^\alpha = E^{J\pi\alpha} \sum_{K'b} \langle Q^{(a)} | \tilde{P}_{KK'}^{J\pi} \tilde{P}^{\mathbf{P}=0} | Q^{(b)} \rangle \cdot c_{K'b}^\alpha$$

${}^3\text{He}(\alpha, \gamma){}^7\text{Be}$ radiative capture

one of the key reactions in the solar pp-chains



Effective Nucleon-Nucleon interaction:

UCOM(SRG) $\alpha = 0.20 \text{ fm}^4 - \lambda \approx 1.5 \text{ fm}^{-1}$

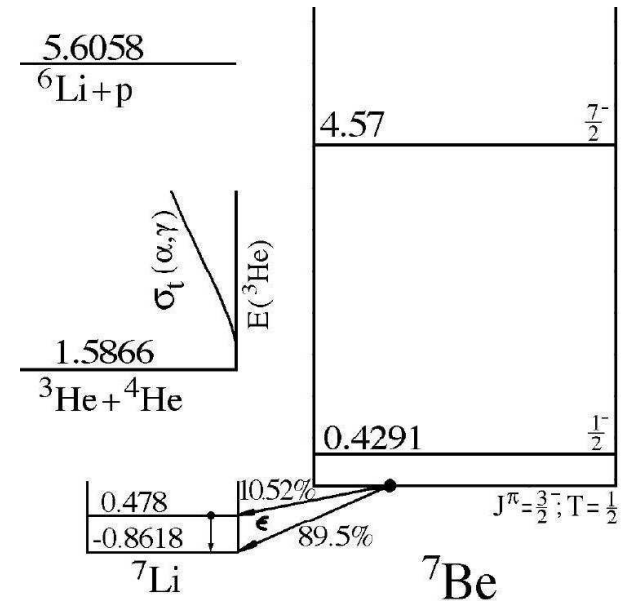
Many-Body Approach:

Fermionic Molecular Dynamics

- Internal region: VAP configurations with radius constraint
- External region: Brink-type cluster configurations
- Matching to Coulomb solutions: Microscopic R -matrix method

Results:

- ${}^7\text{Be}$ bound and scattering states
- Astrophysical S -factor



${}^3\text{He}(\alpha, \gamma){}^7\text{Be}$

FMD model space

Frozen configurations

- antisymmetrized wave function built with ${}^4\text{He}$ and ${}^3\text{He}$ FMD clusters up to channel radius $a=12$ fm

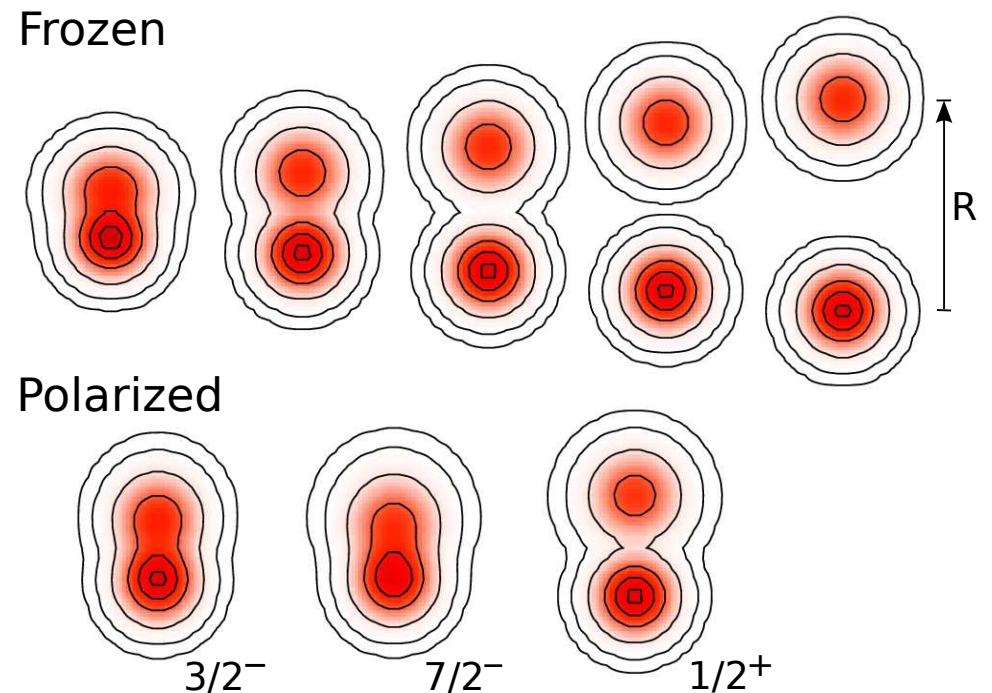
Polarized configurations

- FMD wave functions obtained by VAP on $1/2^-$, $3/2^-$, $5/2^-$, $7/2^-$ and $1/2^+$, $3/2^+$ and $5/2^+$ combined with radius constraint in the interaction region

Boundary conditions

- Match relative motion of clusters at channel radius to Whittaker/Coulomb functions with the **microscopic R-matrix** method of the Brussels group

D. Baye, P.-H. Heenen, P. Descouvemont



• p -wave Bound and Scattering States

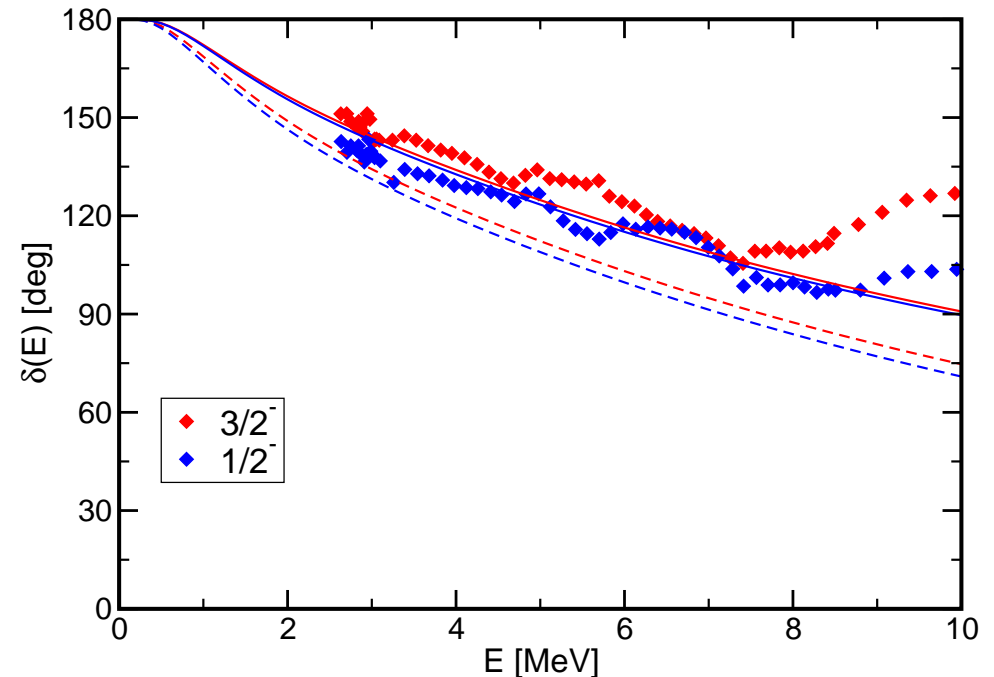
Bound states

		Experiment	FMD
${}^7\text{Be}$	$E_{3/2-}$	-1.59 MeV	-1.49 MeV
	$E_{1/2-}$	-1.15 MeV	-1.31 MeV
	r_{ch}	2.647(17) fm	2.67 fm
	Q	-	-6.83 e fm ²
${}^7\text{Li}$	$E_{3/2-}$	-2.467 MeV	-2.39 MeV
	$E_{1/2-}$	-1.989 MeV	-2.17 MeV
	r_{ch}	2.444(43) fm	2.46 fm
	Q	-4.00(3) e fm ²	-3.91 e fm ²

- centroid of bound state energies well described if polarized configurations included
- tail of wave functions tested by charge radii and quadrupole moments

Phase shift analysis:

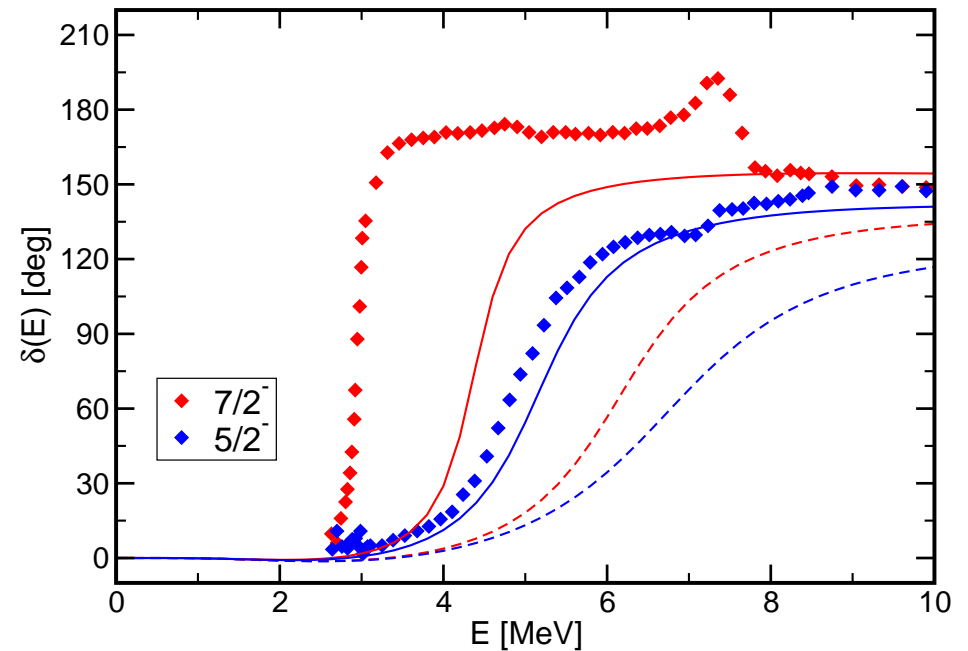
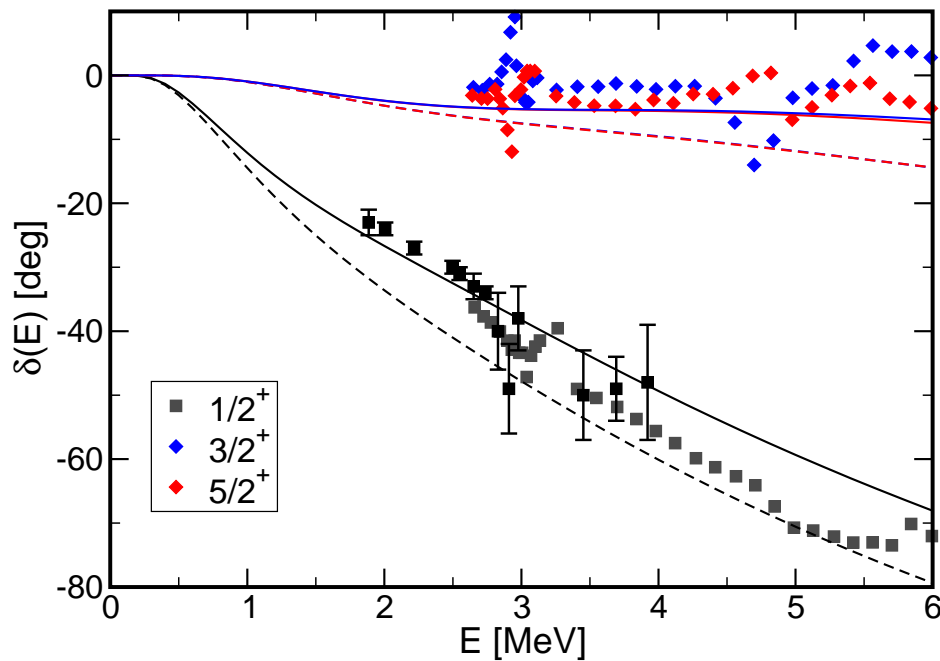
Spiger and Tombrello, PR **163**, 964 (1967)



dashed lines – frozen configurations only
solid lines – polarized configurations in interaction region included

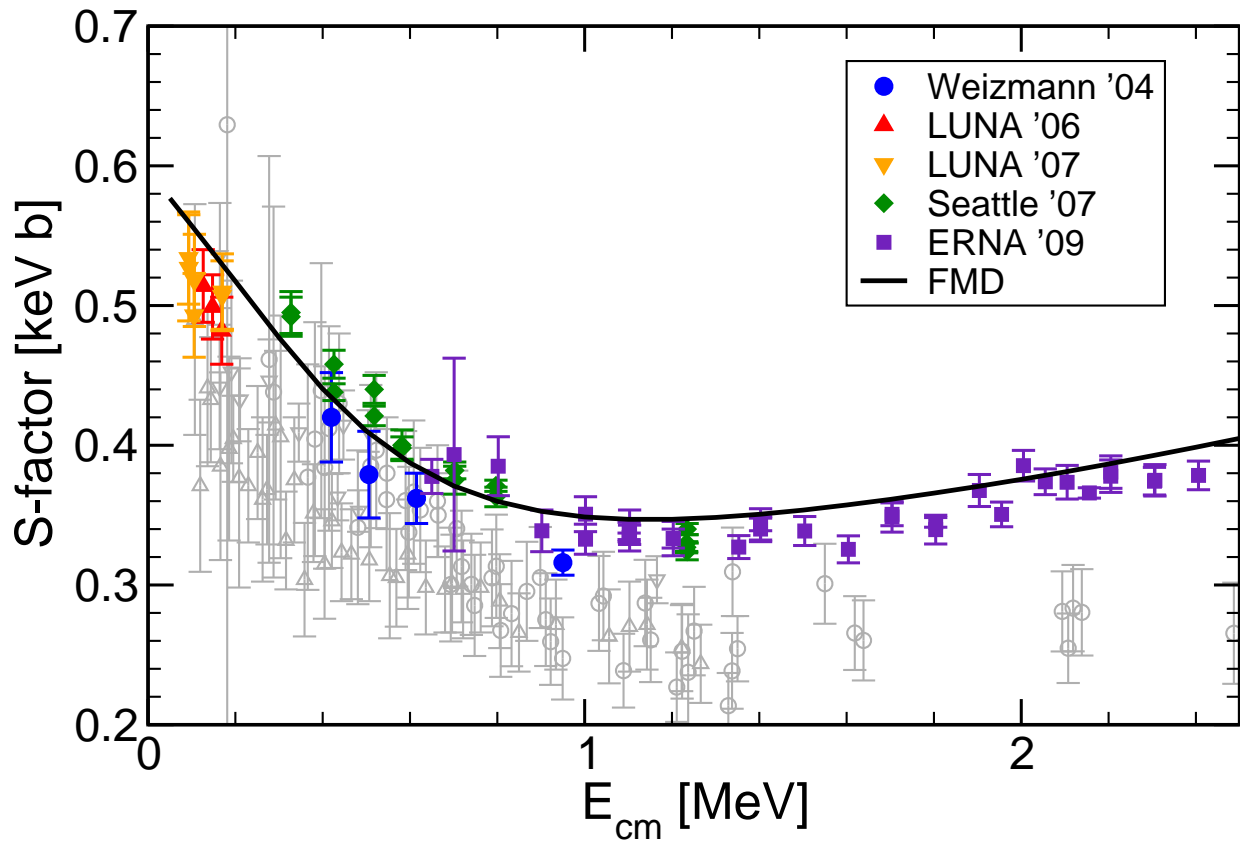
- Scattering phase shifts well described, polarization effects important

- ${}^3\text{He}(\alpha, \gamma){}^7\text{Be}$
- s -, d - and f -wave Scattering States



dashed lines – frozen configurations only – solid lines – FMD configurations in interaction region included

- polarization effects important
- s - and d -wave scattering phase shifts well described
- $7/2^-$ resonance too high, $5/2^-$ resonance roughly right, consistent with no-core shell model calculations



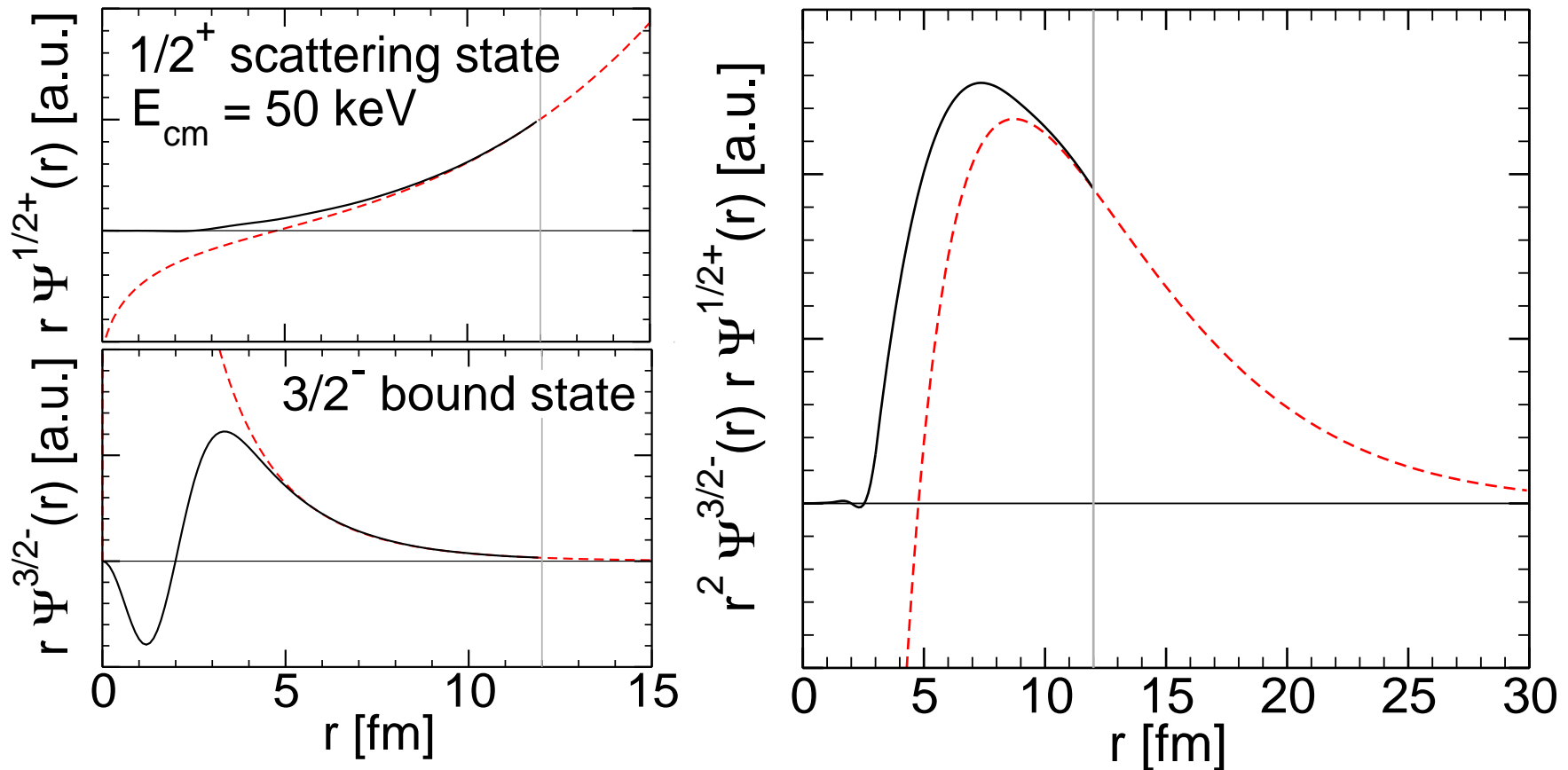
S-factor:

$$S(E) = \sigma(E)E \exp\{2\pi\eta\}$$
$$\eta = \frac{\mu Z_1 Z_2 e^2}{k}$$

Nara Singh *et al.*, PRL **93**, 262503 (2004)
Bemmerer *et al.*, PRL **97**, 122502 (2006)
Confortola *et al.*, PRC **75**, 065803 (2007)
Brown *et al.*, PRC **76**, 055801 (2007)
Di Leva *et al.*, PRL **102**, 232502 (2009)

- dipole transitions from $1/2^+$, $3/2^+$, $5/2^+$ scattering states into $3/2^-$, $1/2^-$ bound states
- FMD is the only model that describes well the energy dependence and normalization of new high quality data
- fully microscopic calculation, bound and scattering states are described consistently

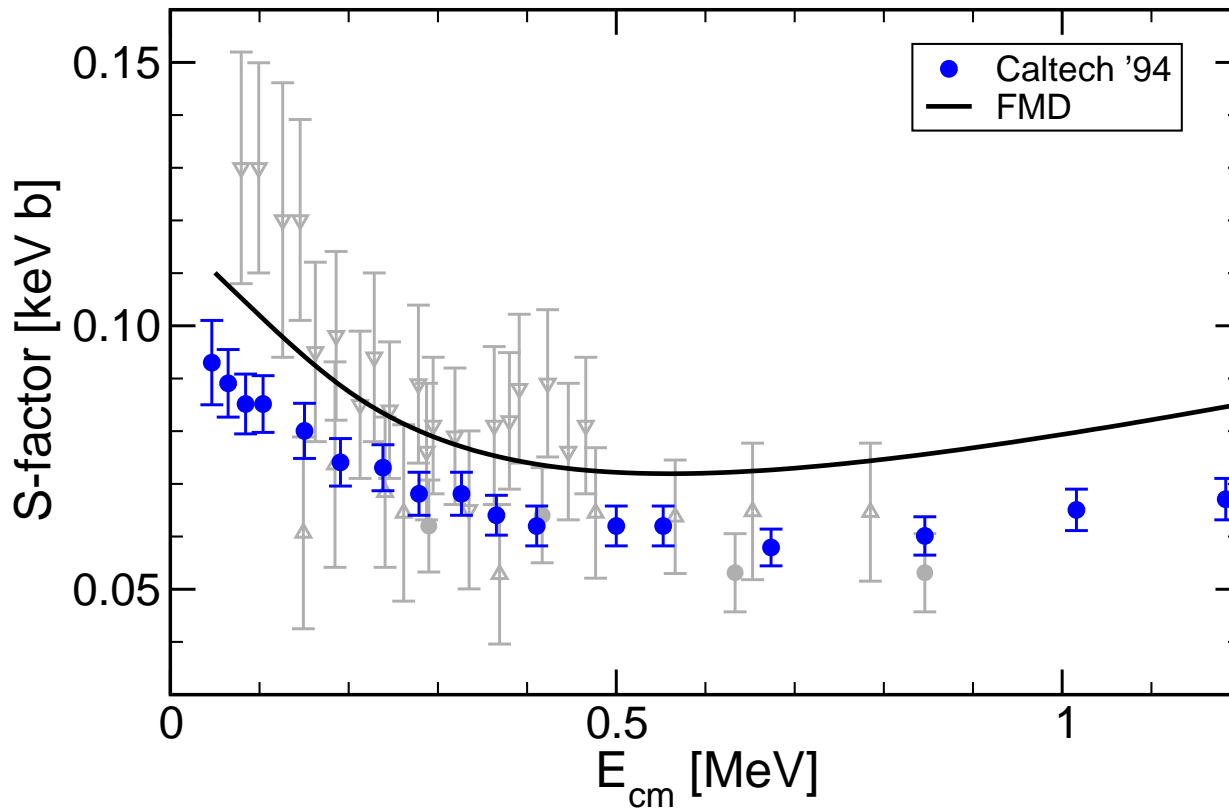
Overlap Functions and Dipole Matrixelements



- Overlap functions from projection on RGM-cluster states
- Coulomb and Whittaker functions matched at channel radius $a=12$ fm
- Dipole matrix elements calculated from overlap functions reproduce full calculation within 2%
- cross section depends significantly on internal part of wave function, description as an “external” capture is too simplified

${}^3\text{H}(\alpha, \gamma){}^7\text{Li}$

S-Factor



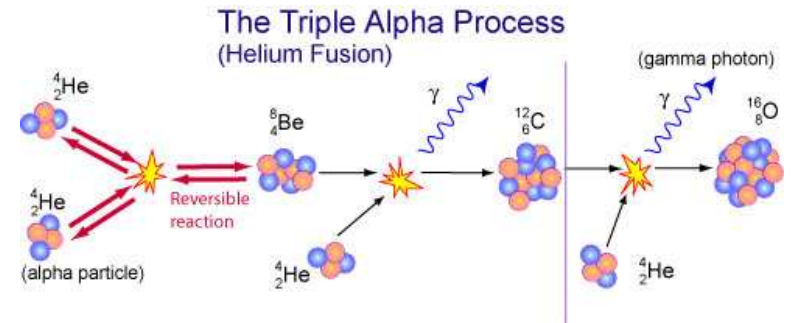
S-factor:

$$S(E) = \sigma(E)E \exp\{2\pi\eta\}$$
$$\eta = \frac{\mu Z_1 Z_2 e^2}{k}$$

Brune *et al.*, PRC **50**, 2205 (1994)

- isospin mirror reaction of ${}^3\text{He}(\alpha, \gamma){}^7\text{Be}$
- ${}^7\text{Li}$ bound state properties and phase shifts well described
- ➔ FMD calculation describes energy dependence of Brune *et al.* data but cross section is larger by about 15%

Cluster States in ^{12}C

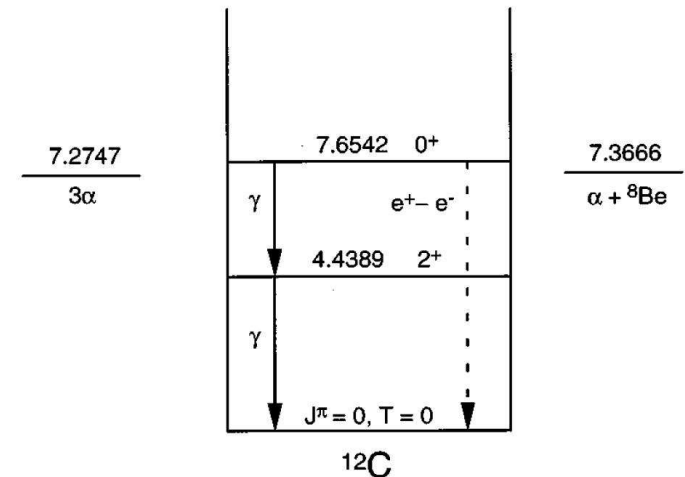


Astrophysical Motivation

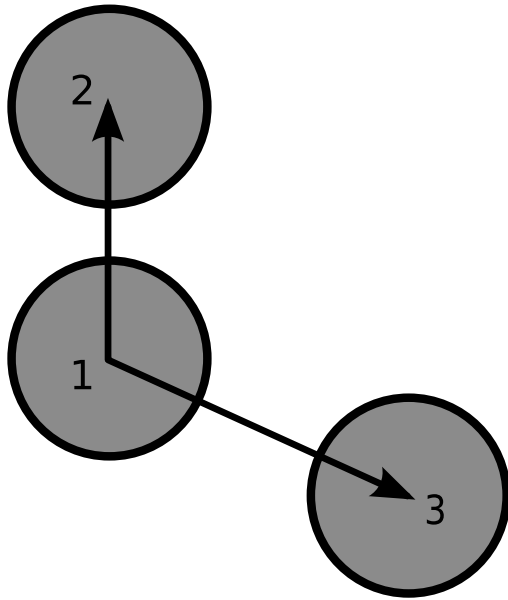
- Helium burning: triple alpha-reaction

Structure

- Is the Hoyle state a pure α -cluster state ?
- Other excited 0^+ and 2^+ states
- ➔ Compare FMD results to microscopic α -cluster model
- ➔ Intrinsic structure from two-body densities
- ➔ Analyze wave functions in harmonic oscillator basis



Microscopic α -Cluster Model



$$R_{12} = (2, 4, \dots, 10) \text{ fm}$$

$$R_{13} = (2, 4, \dots, 10) \text{ fm}$$

$$\cos(\vartheta) = (1.0, 0.8, \dots, -1.0)$$

altogether 165 configurations

Basis States

- describe Hoyle State as a system of 3 ^4He nuclei

$$|\psi_{3\alpha}(\mathbf{R}_1, \mathbf{R}_2, \mathbf{R}_3); JMK\pi\rangle = P_{MK}^J P^\pi \mathcal{A} \{ |\psi_\alpha(\mathbf{R}_1)\rangle \otimes |\psi_\alpha(\mathbf{R}_2)\rangle \otimes |\psi_\alpha(\mathbf{R}_3)\rangle \}$$

Volkov Interaction

- simple central interaction
- parameters adjusted to give reasonable α binding energy and radius, α – α scattering data, adjusted to reproduce ^{12}C ground state energy

✗ only reasonable for ^4He , ^8Be and ^{12}C nuclei

'BEC' wave functions

- interpretation of the Hoyle state as a Bose-Einstein Condensate of α -particles by Funaki, Tohsaki, Horiuchi, Schuck, Röpke
- same interaction and α -cluster parameters used

Cluster States in ^{12}C

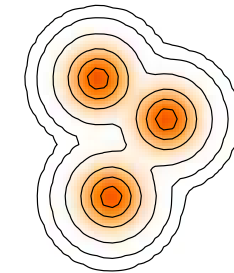
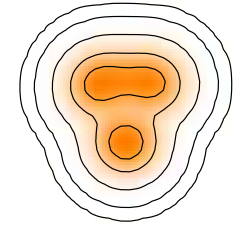
FMD

Basis States

- 20 FMD states obtained in Variation after Projection on 0^+ and 2^+ with constraints on the radius
- 42 FMD states obtained in Variation after Projection on parity with constraints on radius and quadrupole deformation
- 165 α -cluster configurations
- projected on angular momentum and linear momentum

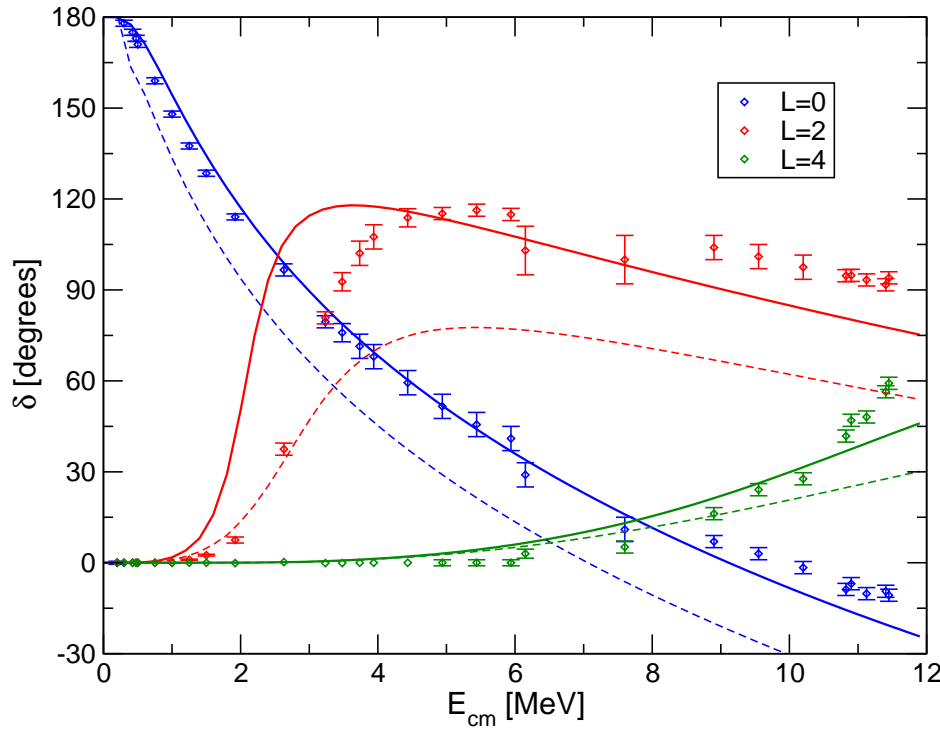
Interaction

- UCOM interaction ($I_9=0.30 \text{ fm}^3$ with phenomenological two-body correction term (momentum-dependent central and spin-orbit) fitted to doubly-magic nuclei
- not tuned for α - α scattering or ^{12}C properties

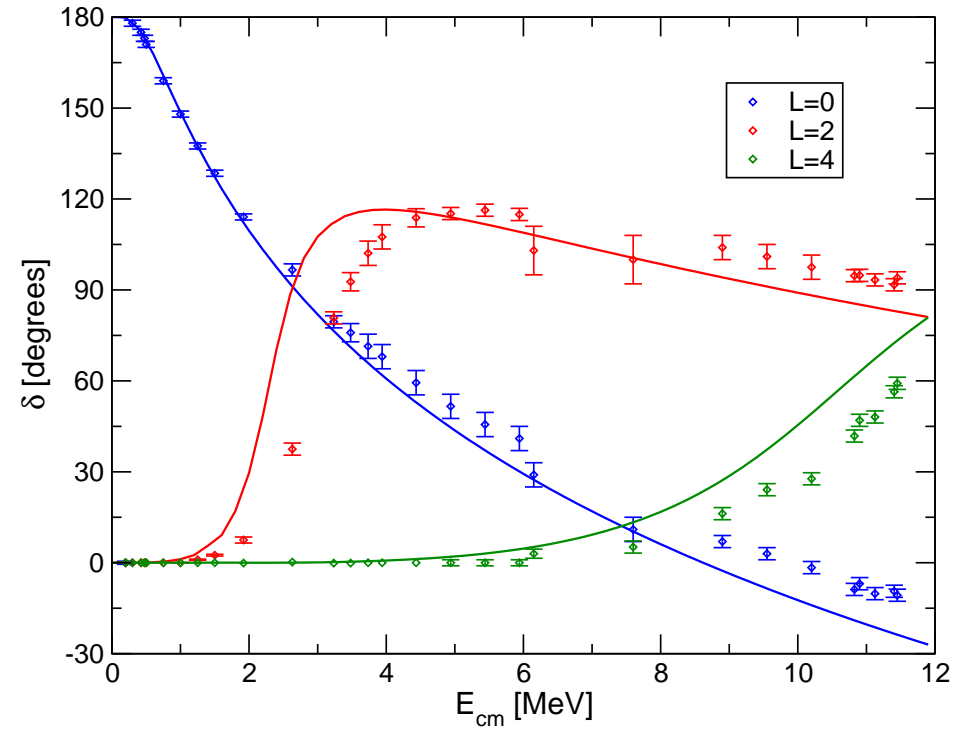


Cluster States in ^{12}C α - α Phaseshifts

FMD



Cluster Model

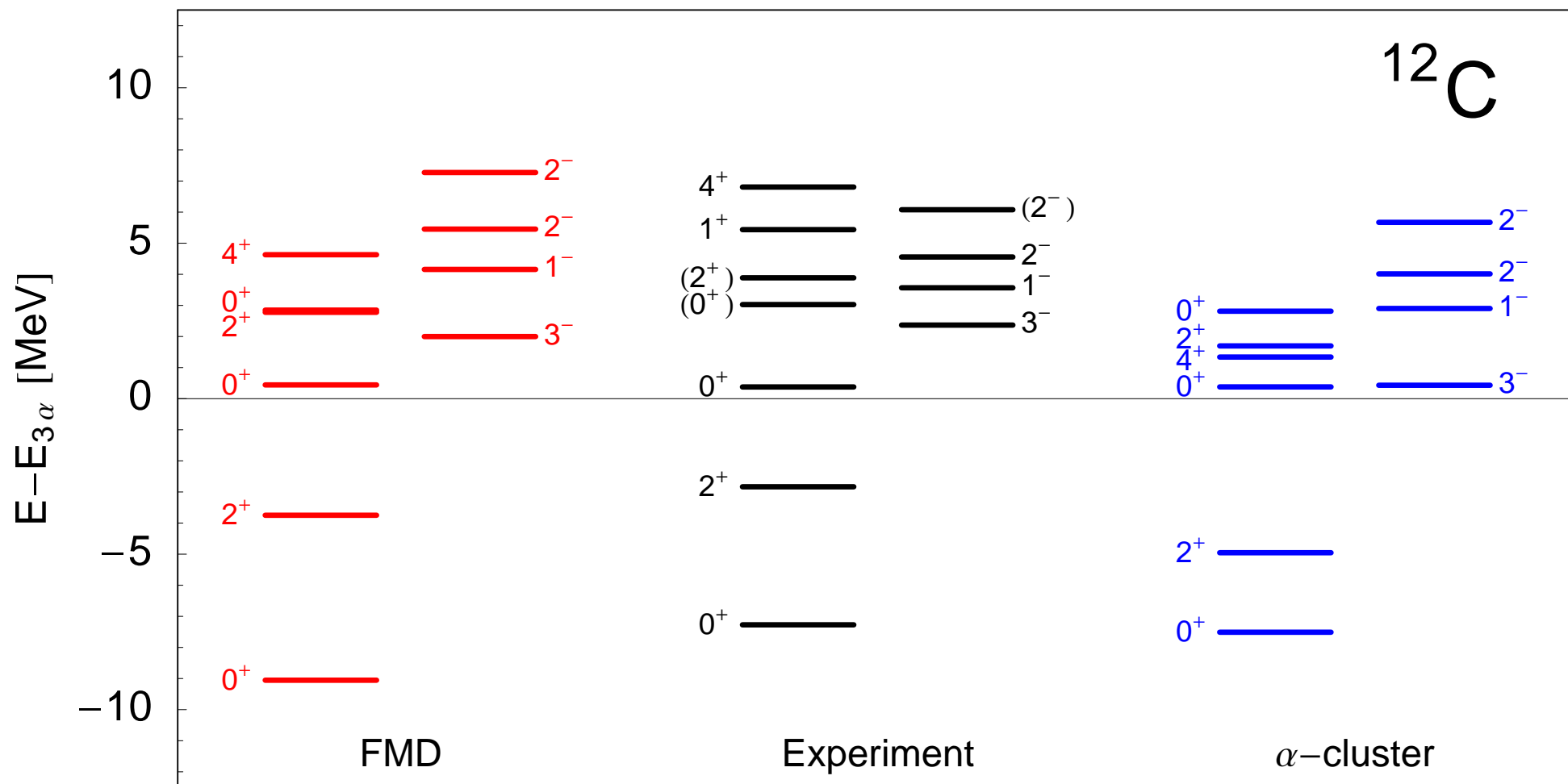


- Phaseshifts calculated with cluster configurations only (dashed lines)
- Phaseshifts calculated with additional FMD VAP configurations in the interaction region (solid lines)

- only cluster configurations included

➔ similar quality for description of α - α -scattering

Cluster States in ^{12}C Comparison



Cluster States in ^{12}C Comparison

	Exp ¹	Exp ²	FMD	α -cluster	'BEC' ³
$E(0_1^+)$	-92.16		-92.64	-89.56	-89.52
$E^*(2_1^+)$	4.44		5.31	2.56	2.81
$E(3\alpha)$	-84.89		-83.59	-82.05	-82.05
$E(0_2^+) - E(3\alpha)$	0.38		0.43	0.38	0.26
$E(0_3^+) - E(3\alpha)$	(3.0)	2.7(3)	2.84	2.81	
$E(2_2^+) - E(3\alpha)$	(3.89)	2.6(3)	2.77	1.70	
$r_{\text{charge}}(0_1^+)$	2.47(2)		2.53	2.54	
$r(0_1^+)$			2.39	2.40	2.40
$r(0_2^+)$			3.38	3.71	3.83
$r(0_3^+)$			4.62	4.75	
$r(2_1^+)$			2.50	2.37	2.38
$r(2_2^+)$			4.43	4.02	
$M(E0, 0_1^+ \rightarrow 0_2^+)$	5.4(2)		6.53	6.52	6.45
$B(E2, 2_1^+ \rightarrow 0_1^+)$	7.6(4)		8.69	9.16	
$B(E2, 2_1^+ \rightarrow 0_2^+)$	2.6(4)		3.83	0.84	
$B(E2, 2_2^+ \rightarrow 0_1^+)$?		0.46	1.99	

experimental situation for 0_3^+ and 2_2^+ states still unsettled (?)

2_2^+ resonance at 1.8 MeV above threshold included in NACRE compilation

¹ Ajzenberg-Selove, Nuc. Phys. **A506**, 1 (1990)

² Itoh et al., Nuc. Phys. **A738**, 268 (2004)

³ Funaki et al., Phys. Rev. C **67**, 051306(R) (2003)

Cluster States in ^{12}C Comparison

	Exp ¹	Exp ²	FMD	α -cluster	'BEC' ³
$E(0_1^+)$	-92.16		-92.64	-89.56	-89.52
$E^*(2_1^+)$	4.44		5.31	2.56	2.81
$E(3\alpha)$	-84.89		-83.59	-82.05	-82.05
$E(0_2^+) - E(3\alpha)$	0.38		0.43	0.38	0.26
$E(0_3^+) - E(3\alpha)$	(3.0)	2.7(3)	2.84	2.81	
$E(2_2^+) - E(3\alpha)$	(3.89)	2.6(3)	2.77	1.70	
$r_{\text{charge}}(0_1^+)$	2.47(2)		2.53	2.54	
$r(0_1^+)$			2.39	2.40	2.40
$r(0_2^+)$			3.38	3.71	3.83
$r(0_3^+)$			4.62	4.75	
$r(2_1^+)$			2.50	2.37	2.38
$r(2_2^+)$			4.43	4.02	
$M(E0, 0_1^+ \rightarrow 0_2^+)$	5.4(2)		6.53	6.52	6.45
$B(E2, 2_1^+ \rightarrow 0_1^+)$	7.6(4)		8.69	9.16	
$B(E2, 2_1^+ \rightarrow 0_2^+)$	2.6(4)		3.83	0.84	
$B(E2, 2_2^+ \rightarrow 0_1^+)$?		0.46	1.99	

experimental situation for 0_3^+ and 2_2^+ states still unsettled (?)

2_2^+ resonance at 1.8 MeV above threshold included in NACRE compilation

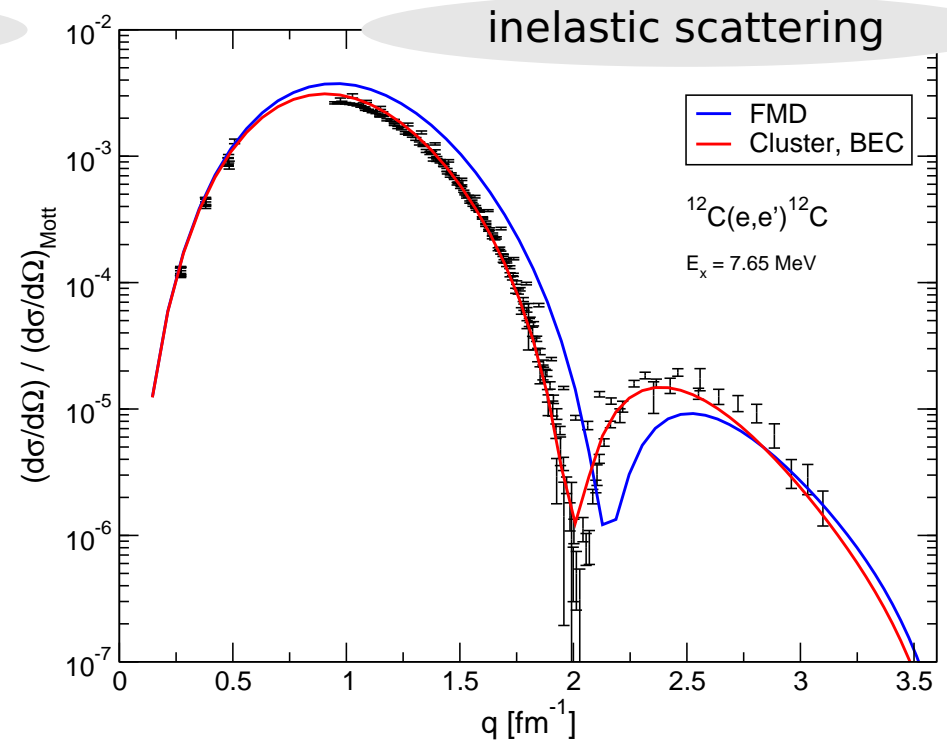
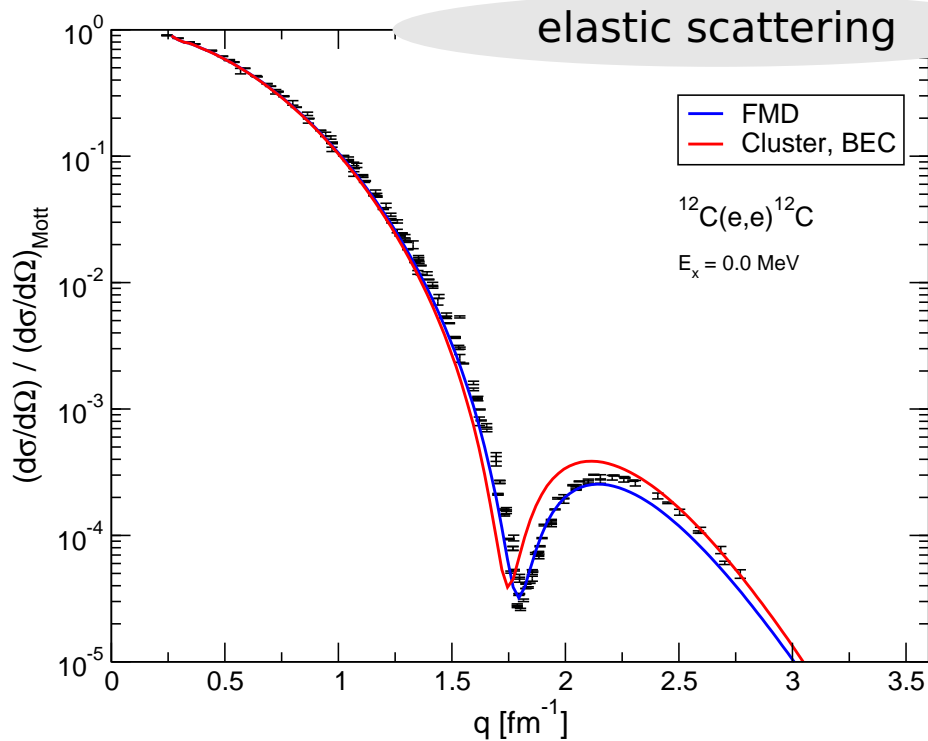
calculated in bound state approximation

¹ Ajzenberg-Selove, Nuc. Phys. **A506**, 1 (1990)

² Itoh et al., Nuc. Phys. **A738**, 268 (2004)

³ Funaki et al., Phys. Rev. C **67**, 051306(R) (2003)

Cluster States in ^{12}C Electron Scattering Data



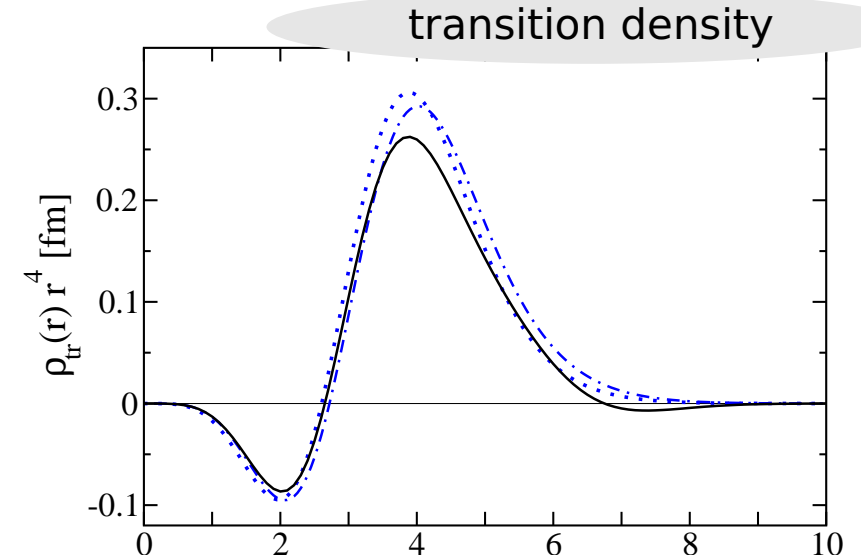
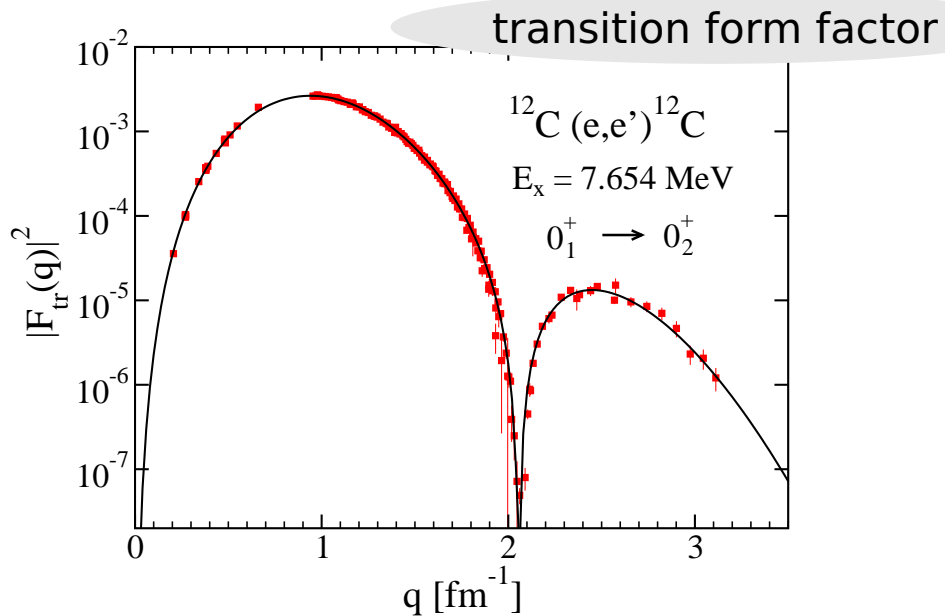
- compare with precise electron scattering data up to high momenta in Distorted Wave Born Approximation
- use intrinsic density

$$\rho(\mathbf{x}) = \sum_{k=1}^A \langle \Psi | \delta(\mathbf{x}_k - \mathbf{X} - \mathbf{x}) | \Psi \rangle$$

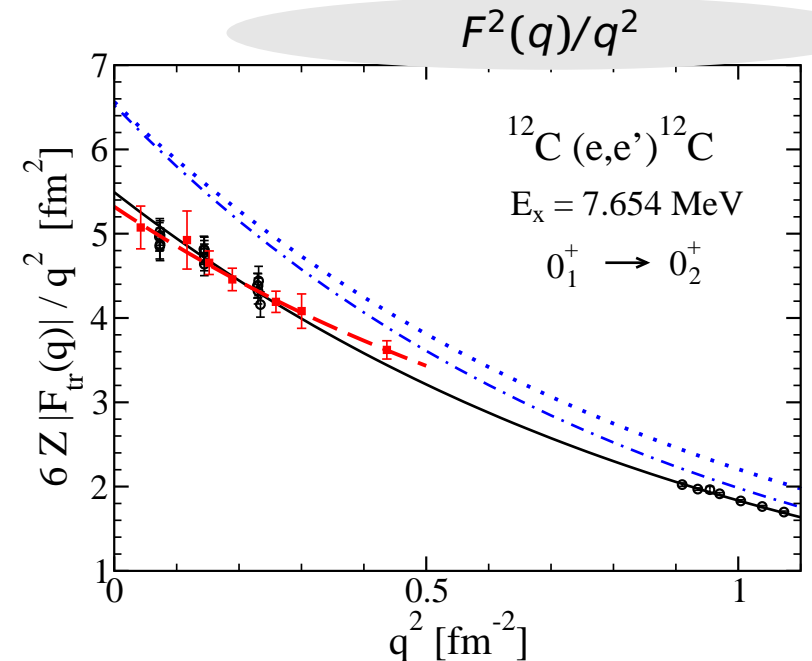
- ➔ elastic cross section described very well by FMD
- ➔ transition cross section better described by cluster model

Cluster States in ^{12}C

Monopole Matrix Element

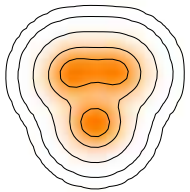


- $M(E0)$ determines the pair decay width
- model-independent self-consistent determination of transition form-factor/density in DWBA
- data at high momentum transfer necessary to constrain $M(E0)$ matrix element

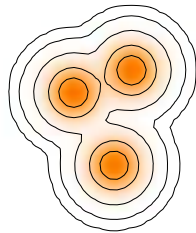


Cluster States in ^{12}C Important Configurations

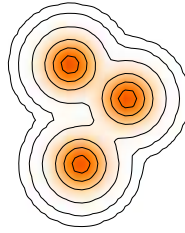
- Calculate the overlap with FMD basis states to find the most important contributions to the Hoyle state



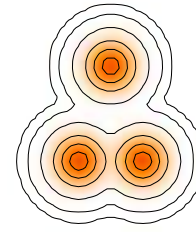
$$\begin{aligned} |\langle \cdot | 0_1^+ \rangle| &= 0.94 \\ |\langle \cdot | 2_1^+ \rangle| &= 0.93 \end{aligned}$$



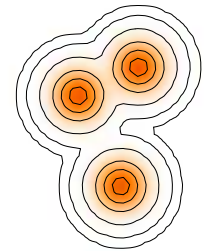
$$|\langle \cdot | 0_2^+ \rangle| = 0.72$$



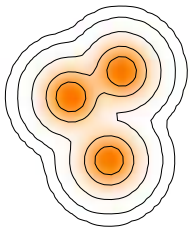
$$|\langle \cdot | 0_2^+ \rangle| = 0.71$$



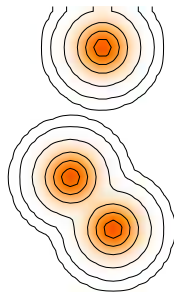
$$|\langle \cdot | 0_2^+ \rangle| = 0.61$$



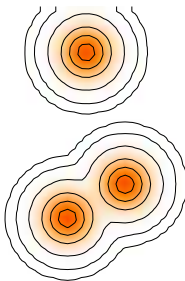
$$|\langle \cdot | 0_2^+ \rangle| = 0.61$$



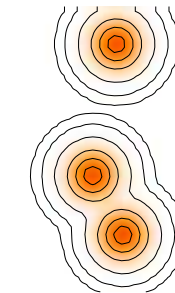
$$|\langle \cdot | 3_1^- \rangle| = 0.83$$



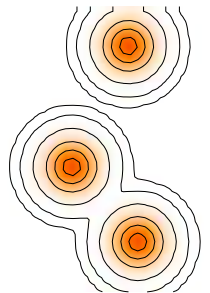
$$|\langle \cdot | 0_3^+ \rangle| = 0.50$$



$$|\langle \cdot | 0_3^+ \rangle| = 0.49$$



$$|\langle \cdot | 0_3^+ \rangle| = 0.44$$

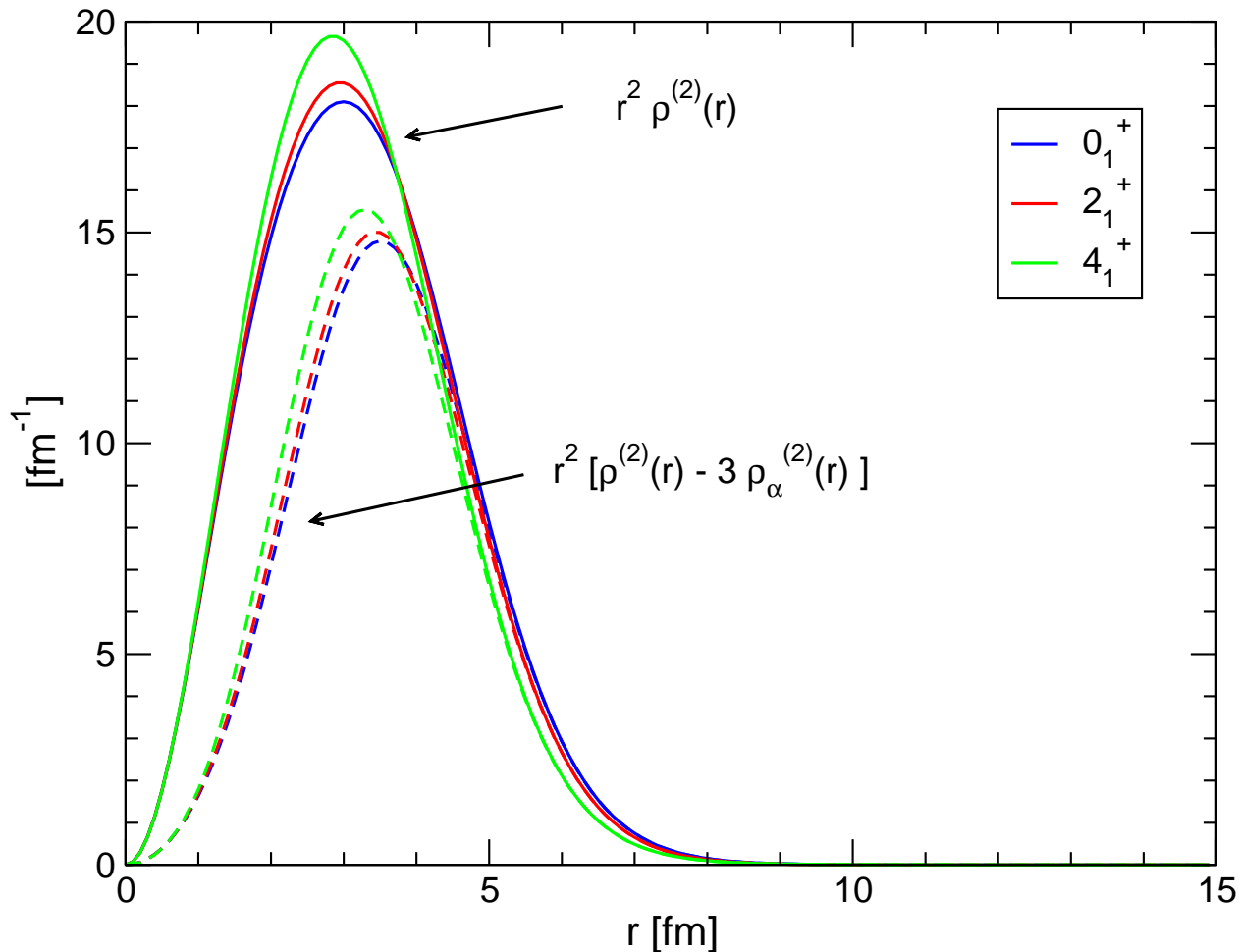


$$|\langle \cdot | 0_3^+ \rangle| = 0.41$$

FMD basis states are not orthogonal!

0_2^+ and 0_3^+ states have no rigid intrinsic structure

ground state band



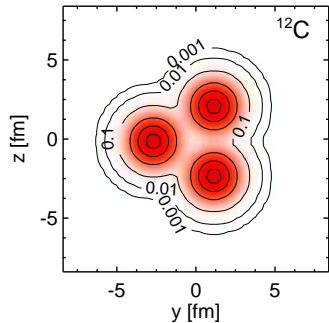
Cluster Model

$$\rho^{(2)}(r) = \langle \Psi | \sum_{i < j} \delta(\mathbf{r} - \mathbf{r}_{ij}) | \Psi \rangle$$

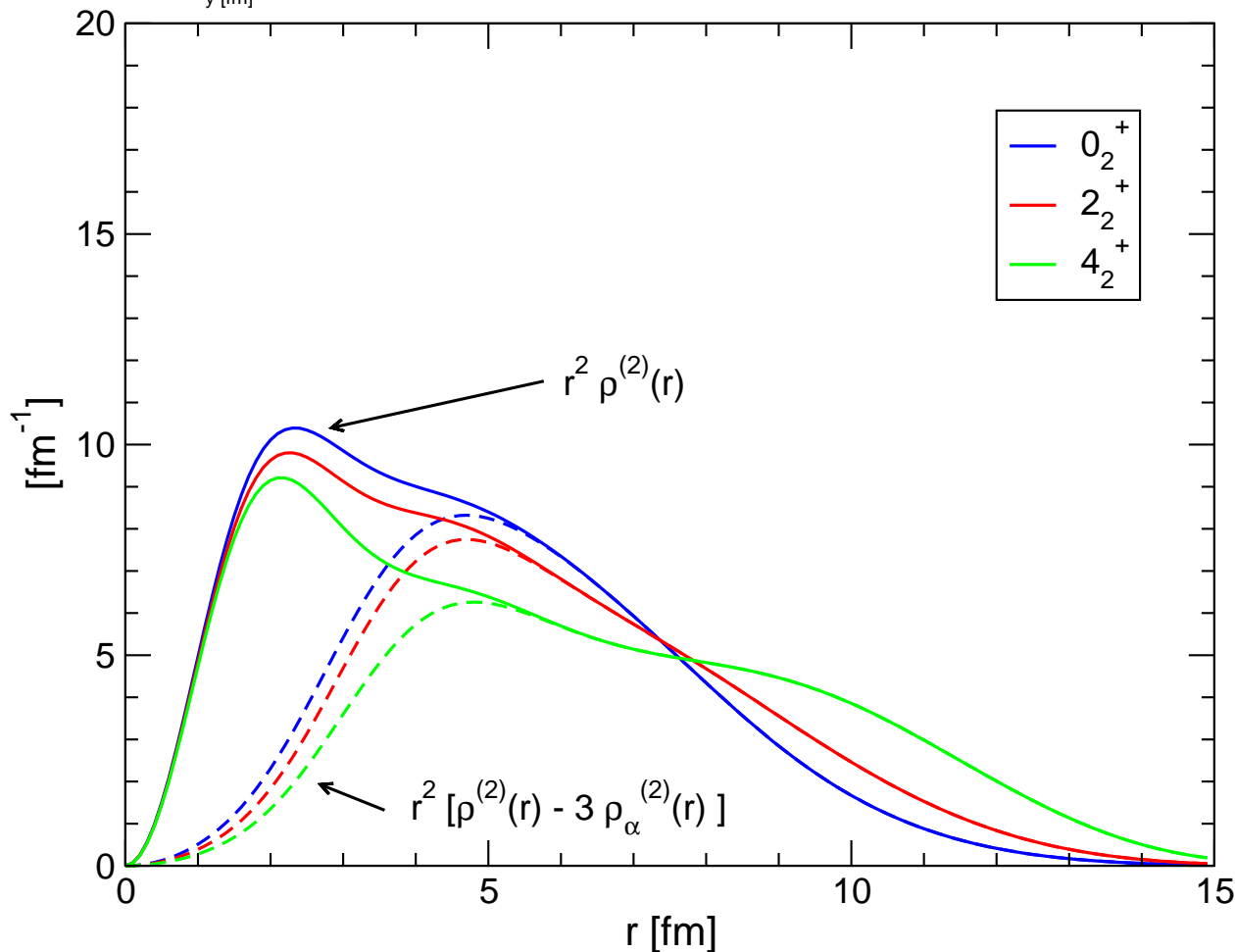
- subtract contributions from α 's to extract " α - α " correlations
- (subtracted) two-body density peaks at 3.5 fm
- ➔ consistent with **compact triangular structure**

Cluster States in ^{12}C

Two-body Densities and Intrinsic Structure



Hoyle state "band"



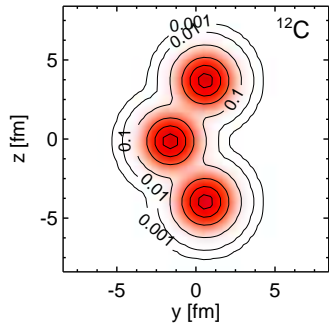
Cluster Model

$$\rho^{(2)}(r) = \langle \Psi | \sum_{i < j} \delta(\mathbf{r} - \mathbf{r}_{ij}) | \Psi \rangle$$

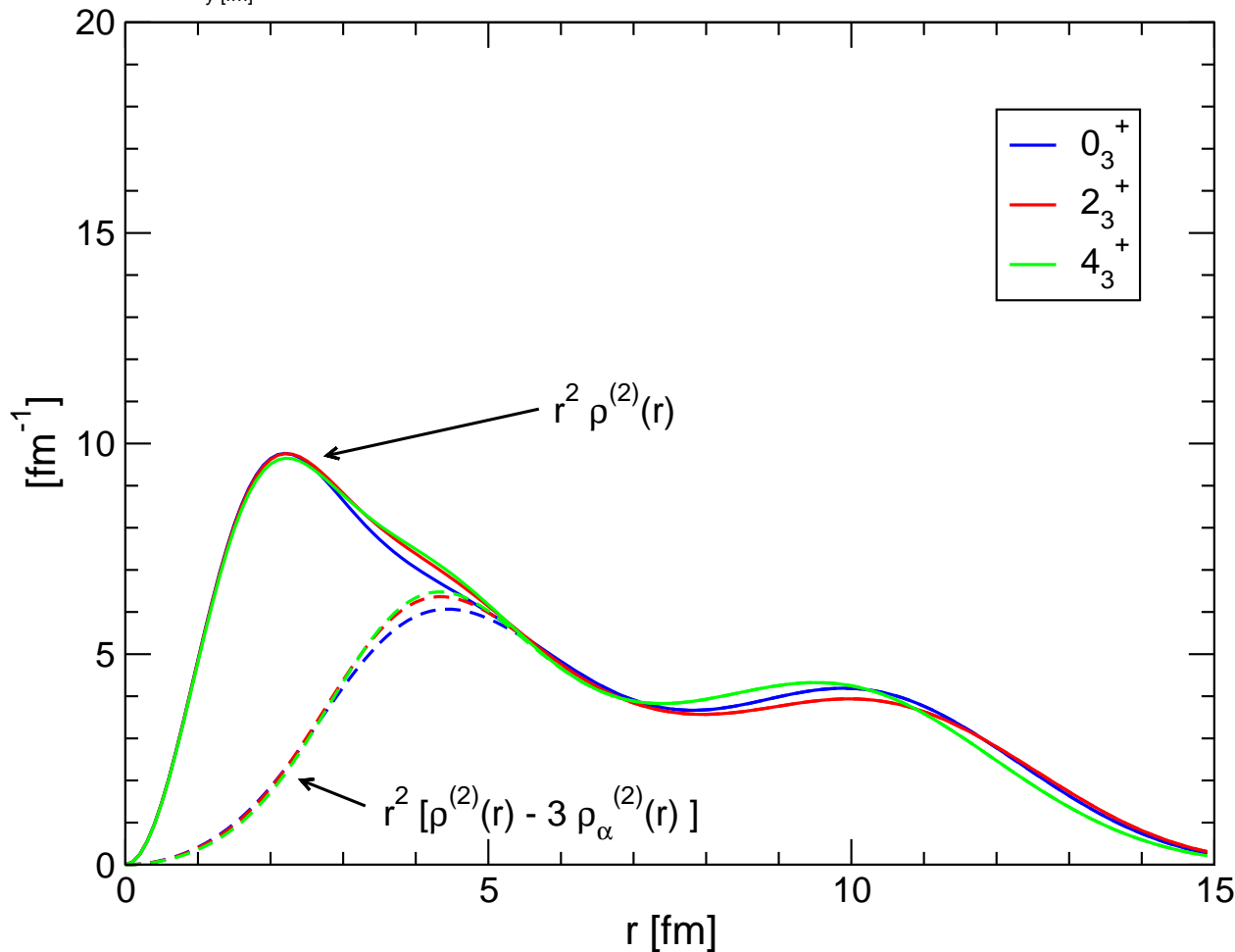
- subtract contributions from α 's to extract " α - α correlations"
- Hoyle state two-body density peaks at 5 fm, extended tail
- consistent with **triangular structure**
- tail in 2_2^+ and 4_2^+ states more pronounced
- admixture of open triangle configurations

Cluster States in ^{12}C

Two-body Densities and Intrinsic Structure



third 0^+ state band

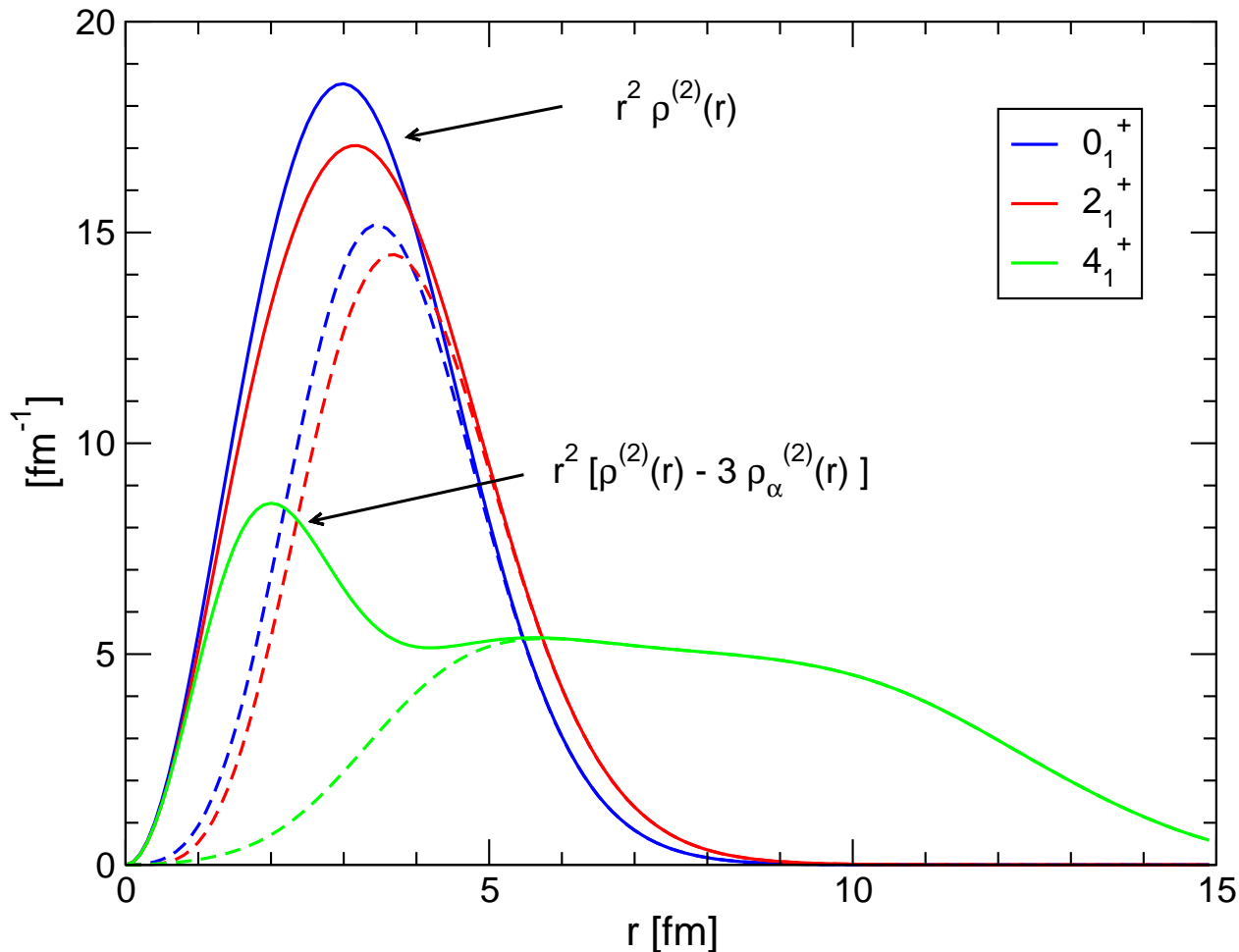


Cluster Model

$$\rho^{(2)}(r) = \langle \Psi | \sum_{i < j} \delta(\mathbf{r} - \mathbf{r}_{ij}) | \Psi \rangle$$

- subtract contributions from α 's to extract " α - α " correlations
- two-body density peaks at 4.5 fm and 10 fm
- ➔ consistent with **open triangle/chain configuration**

ground state band

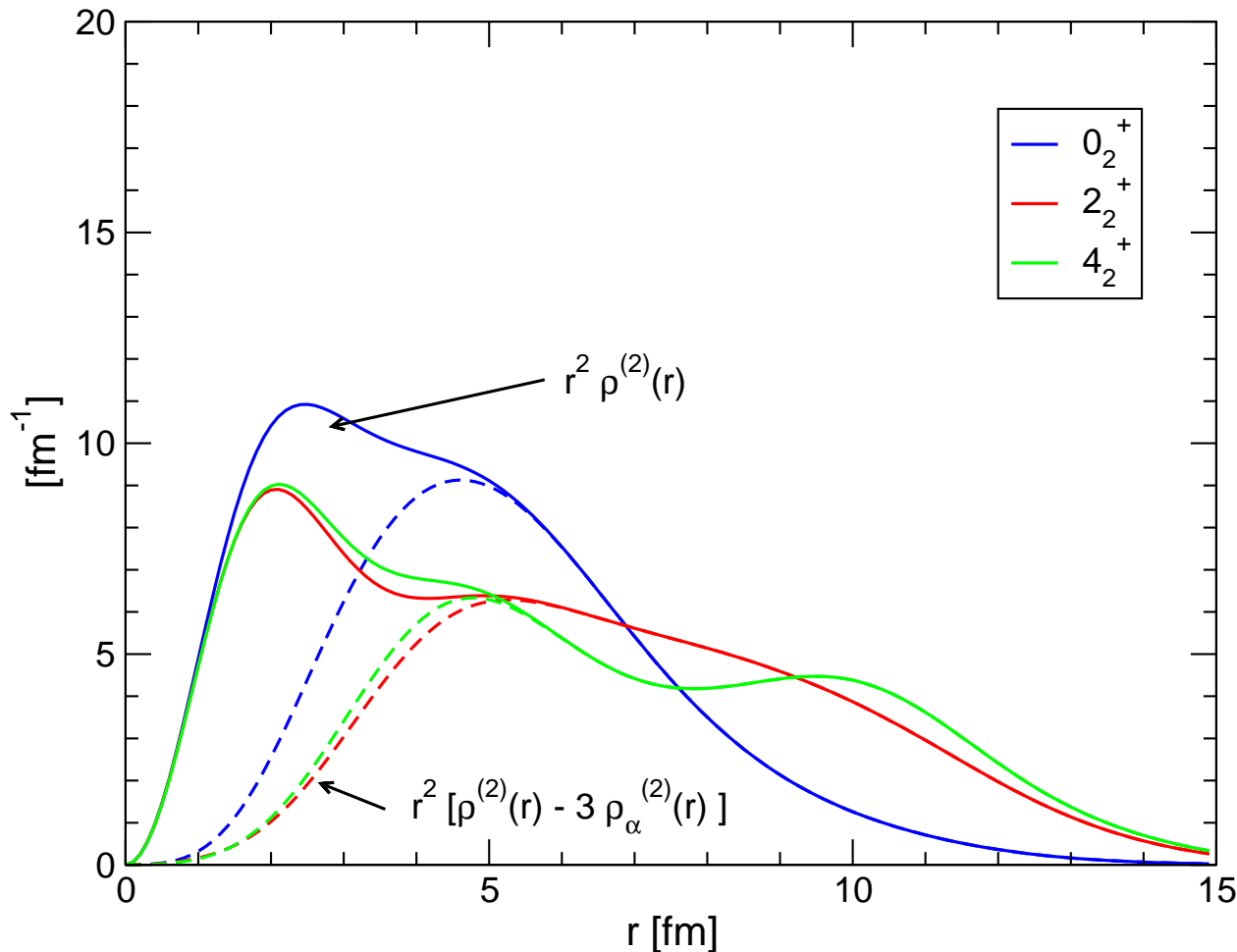


FMD

$$\rho^{(2)}(r) = \langle \Psi | \sum_{i < j} \delta(\mathbf{r} - \mathbf{r}_{ij}) | \Psi \rangle$$

- subtract contributions from α 's to extract α - α correlations
- (corrected) two-body density peaks at 3.5 fm for 0^+ and 2^+
- 4^+ state strongly mixed with cluster configurations

Hoyle state "band"

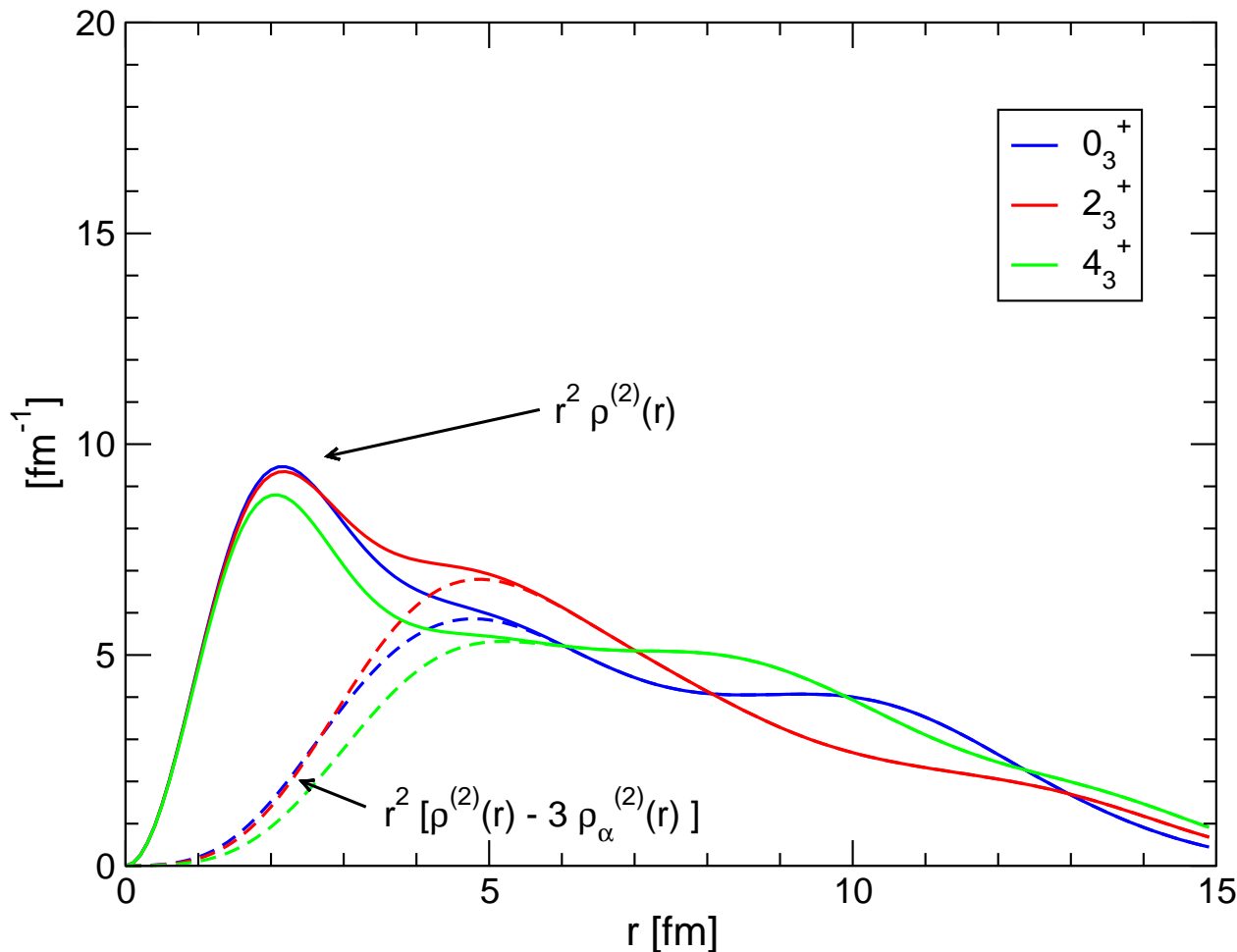


FMD

$$\rho^{(2)}(r) = \langle \Psi | \sum_{i < j} \delta(\mathbf{r} - \mathbf{r}_{ij}) | \Psi \rangle$$

- subtract contributions from α 's to extract α - α correlations
- Hoyle state two-body density peaks at 5 fm, extended tail
- consistent with **extended triangular structure**
- 2_2^+ and 4_2^+ states have different intrinsic structure
- admixture of open triangle configurations

third 0^+ state band



FMD

$$\rho^{(2)}(r) = \langle \Psi | \sum_{i < j} \delta(\mathbf{r} - \mathbf{r}_{ij}) | \Psi \rangle$$

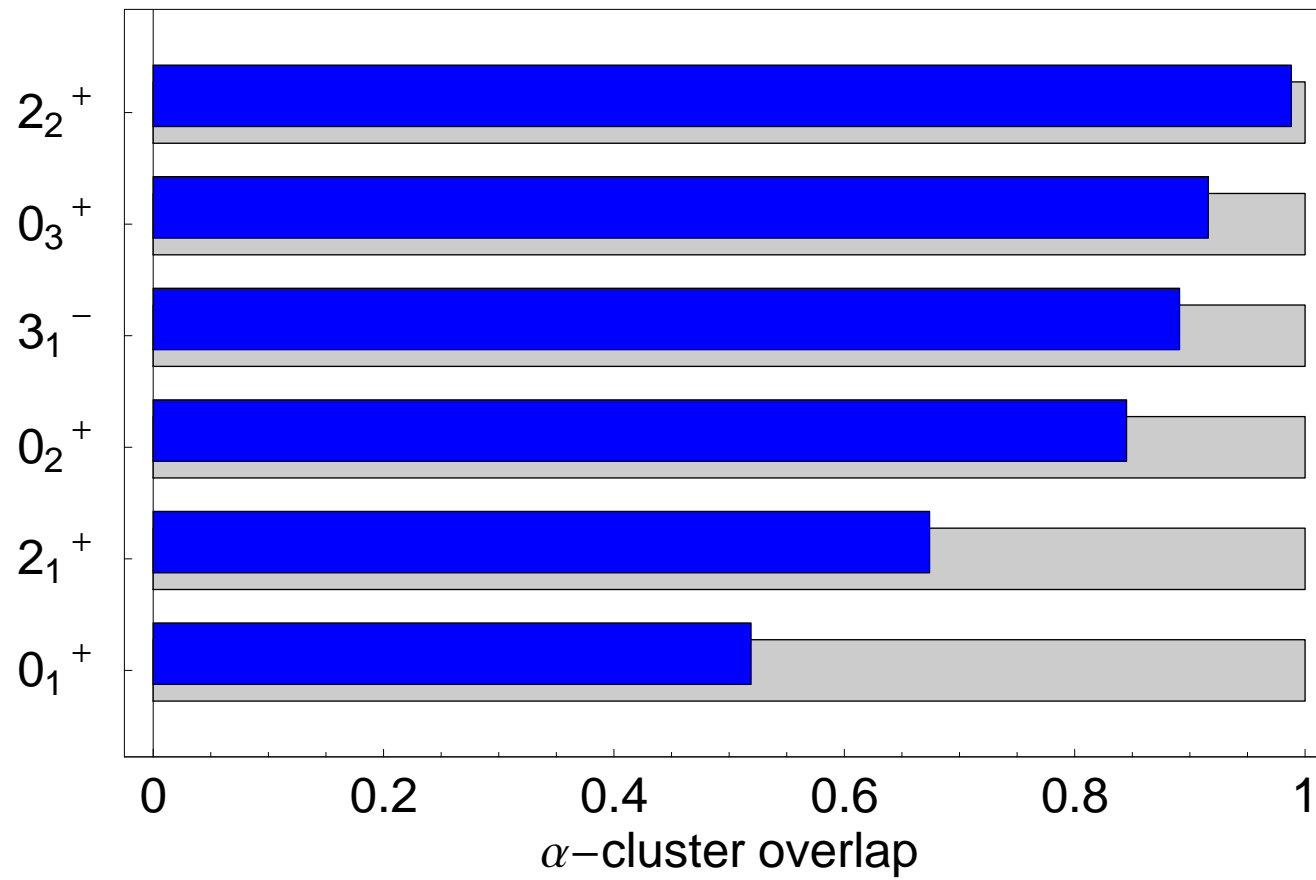
- subtract contributions from α 's to extract α - α correlations
- two-body density peaks at 4.5 fm and 10 fm
- consistent with **chain configuration**

Cluster States in ^{12}C

Overlap with Cluster Model Space

Calculate the overlap of FMD wave functions with pure α -cluster model space

$$N_\alpha = \langle \Psi | P_{3\alpha} | \Psi \rangle$$



Hoyle state has 15%
non-alpha
admixtures

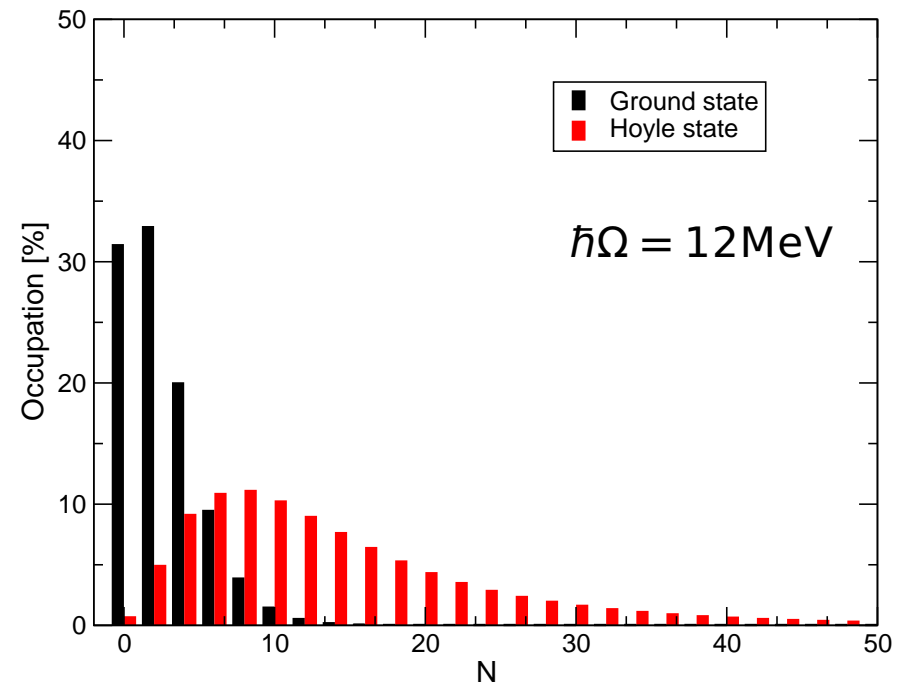
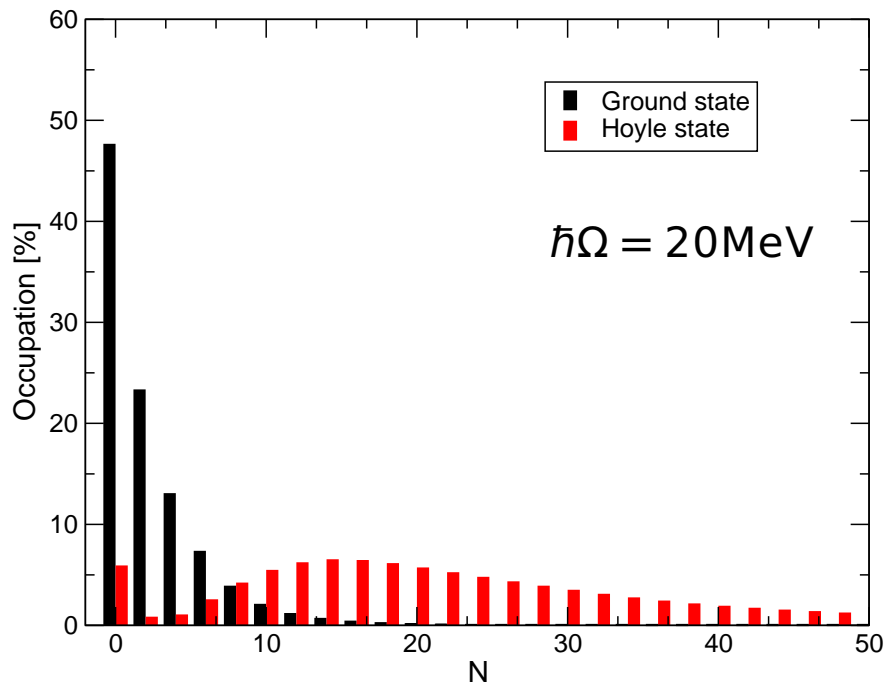
Cluster States in ^{12}C

Harmonic Oscillator $N\hbar\Omega$ Excitations

Y. Suzuki et al., Phys. Rev. C **54** 2073, (1996):

$$\text{Occ}(N) = \langle \Psi | \delta \left(\sum_i (H_i^{\text{HO}} / \hbar\Omega - 3/2) - N \right) | \Psi \rangle$$

Cluster Model



- Hoyle state very difficult to converge in no-core shell model

T. Neff, H. Feldmeier, Few-Body Syst. **45**, 145 (2009)

Summary

Short-range correlations in light nuclei

- short-range and high-momentum behavior of two-body densities identical in $A=2,3,4$ nuclei
- Two-body densities in ${}^4\text{He}$ with SRG evolved interactions

${}^3\text{He}(\alpha,\gamma){}^7\text{Be}$ Radiative Capture

- Bound states, resonance and scattering wave functions
- S-Factor: energy dependence and normalization
- Analyzed in terms of overlap functions

Cluster States in ${}^{12}\text{C}$

- Consistent description of ground state band and Hoyle state
- Investigate Hoyle state structure with electron scattering
- Two-body densities are a model independent tool for investigating structure
- Cluster states need tremendous model space in harmonic oscillator basis

Thanks to my collaborators:

Hans Feldmeier (GSI), Wataru Horiuchi (Hokkaido), Karlheinz Langanke (GSI), Robert Roth (TUD), Yasuyuki Suzuki (Niigata), Dennis Weber (GSI)